NASA TECHNICAL MEMORANDUM

NASA TM-76242

INTERACTION OF THE INTERMEDIATE ENERGY NEUTRINO WITH NUCLEI

E. V. Bugayev, M. A. Rudzskiy, G. S. Bisnovatyy-Kogan, Z. F. Seidov

Translation of "Vzaimodeystviye Neytrino Srednykh Energiy s Yadrami," Academy of Sciences USSR, Institute of Space Research, Moscow, Report Pr-403, 1978, pp. 1-49.

NATIONAL AERONAUTICS AND SPACE ADMINISTRATION
WASHINGTON, D. C. JUNE 1980

STANDARD TITLE PAGE

1. Report No. TM-76242	2. Government Accession No.	3. Recipient's Catalog No.
4. Title and Subtitle INTERACTION OF THE INTERMEDIATE ENERGY NEUTRINO WITH NUCLEI		5. Report Date JUNE 1980 6. Performing Organization Code
7. Author(s) E. V. Bugayev, M. A. Rudzskiy, G. S. Bisnovatyy-Kogan, Z. F. Seidov		8. Performing Organization Report No. 10. Work Unit No.
9. Performing Organization Name and Address SCITRAN Box 5456 Santa Barbara, CA 93108		11. Contract or Grant No. NASW-3198 13. Type of Report and Period Covered Translation
12. Sponsoring Agency Name and Address National Aeronautics and Space Administration Washington, D.C. 20546		14. Sponsoring Agency Code

15. Supplementary Notes

Translation of "Vzaimodeystviye Neytrino Srednykh Energiy s Yadrami," Academy of Sciences USSR, Institute of Space Research, Moscow, Report Pr-403, 1978, pp. 1-49.

16. Abstract

The interaction of the electronic neutrino with nuclei ^{12}C, ^{16}O, ^{37}Cl, ^{56}Fe, ^{71}Ga, ^{81}Br is considered for neutrino energy up to 300 MeV. The nuclei are described by single-particle shell-model with Woods-Saxon potential. The parameters of the potential are specially chosen for each nuclei in order to describe correctly the upper occupied single-particle levels of the nuclei. The cross-sections for inelastic and elastic interactions of neutrino with nuclei are calculated within this model, taking into account charged and neutral current of weak interaction. The neutral currents are described by Weinberg theory. The results of the cross-section calculations are presented and the comparisons with the results of the other authors are given. The possibilities of improvement of the exactness of obtained results are discussed. Some details of the calculations are given in the Appendices.

17. Key Words (Selected by Author(s))	18. Distribution Statement		
	Unclassified - Unlimited		
19. Security Classif. (of this report) Unclassified	20. Security Classif. (of this page) Unclassified	21. No. of Pages 48	22.

NASA-HQ

INTERACTION OF THE INTERMEDIATE ENERGY NEUTRINO WITH NUCLEI

E. V. Bugayev, M. A. Rudzskiy, G. S. Bisnovatyy-Kogan, Z. F. Seidov

1. Introduction

/4*

Many authors have made theoretical studies of the interaction of neutrinos with small and average energies. The research object is usually the transition cross sections in definite states of the finite nuclei, and also the total (with respect to all of the nuclear excitations which are possible for a given neutrino energy) cross sections of the ν-capture. It is usually difficult to calculate the cross section in the energy region $E_\nu \sim 10 - 100$ MeV, where a knowledge of the structure of the low-lying excited states of the target nucleus is very important. Therefore, at present detailed calculations only exist for the simplest ^{12}C [1], [2], ^{16}O [3], [4], ^{37}Cl [5], [6] nuclei. In the energy region which is far from the threshold ($E_\nu > 100$-200 MeV), it is possible to use simple universal models, such as the model of the Fermi-gas [7] and the envelope model of J. Bell and S. Llewellyn Smith (BLS) [8], which use the approximation of completeness.

Further research on the neutrino-nuclear reactions is important for two reasons.

1. The low energy neutrinos play an important role in astrophysics. In the case of steady state combustion, particularly in the case of a collapse, the stars emit neutrinos which can be recorded on the Earth. The energy of the emitted neutrinos in the case of steady state combustion for stars of the main sequence does not exceed 8 MeV, and it may be much greater in the case of a collapse. In the first estimates made by Ya. B. Zel'dovich and

---

*Numbers in the margin indicate pagination in original foreign text.

O. Kh. Guseynov [9], the energy of neutrinos emitted in the case of a collapse was 60 MeV. In the recent calculations of D. K. Nadjozhin, who made the most detailed examination of neutrino processes in the case of collapse, it was found that in the case of diffusion in the nucleus of a star which is not transparent for neutrinos their energy decreases and $E_{\nu_{max}} \sim 20$-30 MeV [10]. /5
The cross section of the ν-capture must be known not only to study the possibilities of recording the neutrinos, but also to study the collapse dynamics. We must also stress that, in principle, there may be fluxes of much higher energy neutrinos having an astrophysical origin, for example, neutrinos from pions which decompose in a year, etc. Thus, the neutrino energy region from the threshold up to approximately 100 MeV is of interest for astrophysics. In this region, as was already noted above, the calculations are very complex and are made for each nucleus individually. Simple nuclear models close to the threshold are not accurate enough, especially for light nuclei.

2. It is known that nuclear targets may be widely used to increase the statistics in accelerator experiments. If the average neutrino energy is not very large (for example, as for the Argonne accelerator, where $E_\nu \gtrsim$ 200-300 MeV), then a detailed study is needed of the effects of the nuclear structure. Within the framework of the shell model of the nucleus, this problem has been studied in [8]. The authors used wave functions of a harmonic oscillator for the calculations, so that they could consider the continuous spectra of the nucleus excitations. The excitation spectrum in this model is far from the real one, and it is difficult to establish the error connected with it. The most detailed calculations at present have been made for the ν-capture reactions in ^{12}C and ^{16}O in [1-4]. They obtained the total cross sections in the neutrino energy range from zero to 500-600 MeV. The article [1] studied the ν-capture by the nucleus ^{12}C. Experimental data were used from 22 low-lying excited states in ^{12}C, obtained from experiments on the electro- and photoexcitation of ^{12}C. Similar calculations were made for the nucleus ^{16}O in [3]. Calculations

were made in [2] of the cross section of semi-lepton processes in nuclei with A = 12 on the basis of the shell model of the nucleus with an oscillator potential hole and allowance for the residual interaction. For agreement with the experimental data, all the transition cross sections had to be reduced, in spite of considering the residual interaction. A similar calculation was made for ^{16}O in [4]. /6

Detailed calculations were made in [1-4] and are only possible for very light, well-studied nuclei. It is extremely complex to perform calculations for heavier nuclei, for example, for ^{37}Cl [6], since the number of low-lying excited states in the nuclei rapidly increases with an increase in their atomic weight A.

The purpose of this article is to formulate a unified method for calculating the cross sections of inelastic neutron-nuclear reactions for the neutrino energy regions from threshold values to approximately 300 MeV. A unified description is given in this region using the precise calculation of all the nuclear transitions described within the framework of a single-frequency shell model with the Wood-Saxon potential (WS). The WS potential has a discrete and continuous spectrum, and gives the correct sequence of single particle levels up to the very heavy nuclei. Since presently it is impossible to give a precise description of the true nuclear states within the framework of this model, to obtain an approximate total transition cross section in all the possible finite states of the nucleus, we calculate the total transition cross section in all the finite single particle states, in which the transitions obey the law of conservation of energy. In real calculations, certain simplifications are made, noted in the second section.

We consider elastic and inelastic reactions with the neutrino electrons:

/7

$$\nu_e + (A,Z) \to e^- + (A,Z+1)^*, \tag{1.1}$$

$$\nu_e + (A,Z) \to \nu_e' + (A,Z)^*, \tag{1.2}$$

$$\nu_e + (A,Z) \to \nu_e' + (A,Z). \tag{1.3}$$

Preliminary results of the calculations were published in [11].

This article consists of four parts and the appendices. The second part gives the derivation of the formulas for the cross sections of the reactions (1.1) - (1.3). The third part discusses the results of calculating the cross sections and makes a comparison with the work of other authors. In conclusion, the methods of improving this procedure are discussed. Certain computational details are examined in the appendices.

2. Interaction cross section in single particle shell model

1. Charged flux

The interaction cross section for a neutrino with a nucleus, accompanied by transitions in an arbitrary group of nuclear states f equals*) (in a laboratory system):

$$d\sigma = \left(\frac{G}{\sqrt{2}}\right)^2 \frac{1}{4k_0 k_0'} \sum_f \left\{ 2\pi \delta(E_i - E_f + q_0)\, \eta_{\mu\nu} J_\mu J_\nu^* \right\} \frac{d\vec{k}'}{(2\pi)^3} \tag{2.1}$$

Here, $\vec{k}, k_0$ and $\vec{k}', k_0'$ are the pulses of the neutrino and electron, respectively; $q = k - k'$, E_i and E_f -- energy of the initial and final nuclei state; $\eta_{\mu\nu}$ -- lepton tensor,

$$\eta_{\mu\nu} = 8\left(k_\mu k_\nu' + k_\nu k_\mu' - \delta_{\mu\nu}(kk') \pm \varepsilon_{\mu\nu\rho\sigma} k_\rho k_\sigma'\right), \tag{2.2}$$

Here J_μ is the 4-vector, determined by the expression /8

*) We use the system of units $\hbar = c = 1$, and the metrics is such that $A^2 = \vec{A}^2 - A_0^2$.

$$J_\mu = J_\mu(\vec{q}) = \int d\vec{x}\, e^{-i\vec{q}\vec{x}} \langle \Psi_f | \hat{J}_\mu(\vec{x}) | \Psi_i \rangle , \qquad (2.3)$$

where $|\Psi_f\rangle$ and $|\Psi_i\rangle$ are the final and initial nuclei states, $\hat{J}_\mu(\vec{x})$ nuclear operator of the flux (see, for example, [12]):

$$\hat{\vec{J}}(\vec{x}) = \sum_i \left\{ \left(\frac{\hat{\vec{p}}_i}{2M} \delta(\vec{x}-\vec{x}_i) + \delta(\vec{x}-\vec{x}_i) \frac{\hat{\vec{p}}_i}{2M} \right) F_1 + \right.$$

$$\left. + \frac{F_1'}{2M} (\vec{\nabla} \times \vec{\sigma}_i) \delta(\vec{x}-\vec{x}_i) + F_A \vec{\sigma}_i \delta(\vec{x}-\vec{x}_i) \right\} \tau_\pm^i + \dots \qquad (2.4)$$

$$\hat{J}_0(\vec{x}) = \sum_i \left\{ F_1 \delta(\vec{x}-\vec{x}_i) + F_A \vec{\sigma}_i \left(\frac{\hat{\vec{p}}_i}{2M} \delta(\vec{x}-\vec{x}_i) + \delta(\vec{x}-\vec{x}_i) \frac{\hat{\vec{p}}_i}{2M} \right) \right\} \tau_\pm^i + \dots$$

In these formulas $\tau_\pm = \frac{1}{2}(\tau_x \pm i\tau_y)$ and σ_i is the Pauli matrix; F_1, F_1' and F_A -- weak form factors of the nucleon (for more details, see the following section); $\hat{\vec{p}}$ -- impulse operator; M -- nucleon mass. Summation is performed over all of the nuclei. Dots mean that the terms $\sim \frac{1}{M^2}$ are omitted, and also corrections for the exchange meson currents. In addition, we have omitted the induced pseudoscalar term (included in the cross section only in terms which are proportional to the lepton mass) and it is assumed there are no currents of the second kind [12].

We are only interested in the cross section which is summed over all the spin and angular variables of the final nuclear system. In this case, we may show (see Appendix A) that the convolution $\eta_{\mu\nu} J_\mu J_\nu^*$ is reduced to the form:

$$\eta_{\mu\nu} J_\mu J_\nu^* = 16 k_0 k_0' \left\{ \left(\frac{q^2}{2q^{*2}} \cos^2\frac{\theta}{2} + \sin^2\frac{\theta}{2} \right) \left(|J_x|^2 + |J_y|^2 \right) + |J_z|^2 \frac{q_0^2}{q^{*2}} \cos^2\frac{\theta}{2} + \right. \qquad (2.5)$$

$$\left. + |J_0|^2 \cos^2\frac{\theta}{2} - 2\mathrm{Re}(J_0 J_z^*) \frac{q_0}{q^*} \cos^2\frac{\theta}{2} \pm (J_x J_y^* - J_y J_x^*) \frac{1}{i} \left(\frac{q^2}{q^{*2}} \cos^2\frac{\theta}{2} + \sin^2\frac{\theta}{2} \right)^{1/2} \right\}.$$

Here θ is the angle between $\vec{k}$ and $\vec{k}'$ (scattering angle), $q^* = |\vec{q}|$ /9
In deriving (2.5), we use a system of coordinates, in which the

vector q is directed along the Z-axis, so that $q^0 = q_Z$. The upper sign corresponds to a reaction with a neutrino; the lower -- with an anti-neutrino.

As was shown in the Introduction, for calculations of the cross section we use a single particle shell model of the nucleus. The nucleus wave function is derived by the unique Slater determinant; the single particle wave functions of the initial and final states -- the corresponding functions of the Woods-Saxon potential belonging to the discrete and continuous spectrum. This model may be immediately applied only to nuclei with filled j-shells. Therefore, in deriving the formulas for the cross section, we only consider these nuclei.

In the single particle model, the components of the vector $J_\mu(\vec{q})$, as is readily found from (2.3), are calculated with the formula:

$$J_\mu(\vec{q}) = \int d\vec{x}\, e^{-i\vec{q}\vec{x}}\, \psi_f^*(\vec{x})\, \hat{J}_\mu\, \psi_i(\vec{x}), \tag{2.6}$$

where ψ_i and ψ_f are the single particle wave functions of the initial and final states; $\hat{J}_\mu$ -- operator,

$$\hat{\vec{J}} = -F_1 \frac{\vec{q}}{2M} - iF_1' \frac{\vec{\sigma}\times\vec{q}}{2M} + F_A\vec{\sigma} + \dots$$

$$\hat{J}_0 = F_1 - F_A \frac{\vec{\sigma}\vec{q}}{2M} + \dots \tag{2.7}$$

The equation (2.7) includes only the terms corresponding to the components left in (2.4). In addition, we use the additional assumption $v/c \ll 1$, where v is the velocity of the initial nucleon in the nucleus. In the nuclei $v/c \lesssim 0.25$, so that the corresponding error is less than 25%. Due to this approximation, in (2.7) there are no terms with a derivative with respect to x, and the /10

calculation includes radial integrals of only the simplest types. The validity of this approximation has been studied, for example, in [13], where it was shown that the discarded terms are only important in a differential cross section for small scattering angles $\theta < 5^{\circ}$.

Following [14], we shall use several modified operators $\hat{J}_\mu$. We shall replace the first component in (2.7) as follows:

$$-F_1 \frac{\vec{q}}{2M} \rightarrow F_1 \frac{q_0}{\vec{q}^2} \vec{q} , \qquad (2.7a)$$

so that the vector part of the operator $\hat{\vec{J}}$ satisfies the law of conservation of the vector current:

$$\hat{\vec{J}}^V \vec{q} = \hat{J}_0^V q_0$$

Let us now calculate in our model of the cross section the reactions (1.1) summed over all the possible energy states of the final nuclear system.

a) Transitions in the discrete spectrum

In this case the integral (2.6) has the form:

$$J_\mu(\vec{q}) = \int d\vec{x}\, e^{-i\vec{q}\vec{x}} \psi_{n_f \ell_f j_f M_f}(\vec{x}) \hat{J}_\mu \psi_{n_i \ell_i j_i M_i}(\vec{x}) \qquad (2.8)$$

The convolution $\eta_{\mu\nu} J_\mu J_\nu^*$ is calculated directly using formula (2.5). The exponent in (2.8), as is customary, is expanded in series in terms of spherical functions, making it possible to separate the radial and angular variables. As a result, we obtain the following expression (details of the calculation are given in Appendix B):

$$\sum_{M_i M_f}\left\{\eta_{\mu\nu}J_\mu J_\nu^*\right\} = 16k_0k_0'(2j_i+1)(2j_f+1)\sum_{J,J'}\left\{(-1)^{\frac{1}{2}(J-J')}\left[\left(\frac{q^2}{q^{*2}}\cos^2\frac{\theta}{2}+\right.\right.\right.$$

$$+2\sin^2\frac{\theta}{2}\left)\left(F_A^2+F_1'^2\frac{q^{*2}}{4M^2}\right)A^1_{JJ'j_ij_f}+\cos^2\frac{\theta}{2}F_1^2\frac{q^4}{q^{*4}}B_{JJ'j_ij_f}+\right.$$

$$+\cos^2\frac{\theta}{2}F_A^2\left(\frac{q_0^2}{q^{*2}}+\frac{q_0}{M}+\frac{q^{*2}}{4M^2}\right)A^0_{JJ'j_ij_f}\mp\frac{2\sin\frac{\theta}{2}}{M}F_1'F_A\cdot \tag{2.9}$$

$$\left.\left.\cdot\left(q^{*2}\sin^2\frac{\theta}{2}+q^2\cos^2\frac{\theta}{2}\right)^{1/2}A^1_{JJ'j_ij_f}\right]R_{n_fl_fj_fJn_il_ij_i}\cdot R_{n_fl_fj_fJ'n_il_ij_i}\right\}.$$

The notation in (2.9) has the following meaning:

$$R_{n_fl_fj_fJn_il_ij_i}\equiv\int_0^\infty R_{n_fl_fj_f}(x)\,j_J(q^*x)R_{n_il_ij_i}(x)\,x^2dx\,, \tag{2.10}$$

where $R_{nlj}(x)$ is the single particle radial wave function; $j_J(x)$ -- spherical Bessel function:

$$A^K_{JJ'j_ij_f}\equiv\sum_C\left\{\langle J01K|CK\rangle\langle J'01K|CK\rangle\left[\langle j_i\tfrac{1}{2}j_f-\tfrac{1}{2}|C0\rangle\right]^2 f(JC)f(J'C)\right\}, \tag{2.11}$$

$$B_{JJ'j_ij_f}\equiv\delta_{JJ'}\left[\langle j_i\tfrac{1}{2}j_f-\tfrac{1}{2}|J0\rangle\right]^2.$$

Here $\langle j_1m_1j_2m_2|jM\rangle$ are the Klebb-Jordan coefficients. Determination of the function $f(JC)$ is given in Appendix B (except for T and C, they also depend on the quantum numbers l, j of the initial and final states).

Let us now use formula (2.1). We shall assume that the response includes the nucleus as a whole (the effective mass of the target equals the nucleus). We thus find (we assume the leptons are

relativistic): /12

$$\frac{d\sigma}{d\Omega} = \left(\frac{G^2}{(2\pi)^2}\right)^2 \frac{1}{8k_0k_0'} k_0'^2 dk_0' \sum_f \left\{ \delta\left(k_0 - k_0' - \frac{q^2}{2M_T} - E^*\right) \sum_{M_i M_f} \left\{ \eta_{\mu\nu} J_\mu J_\nu^* \right\} \right\} =$$

$$= \frac{G^2}{(2\pi)^2} \sum_f \left\{ \frac{k_0'^2}{8k_0k_0'\left(1 + \frac{2k_0}{M_T}\sin^2\frac{\theta}{2}\right)} \sum_{M_i M_f} \left\{ \eta_{\mu\nu} J_\mu J_\nu^* \right\} \right\} \tag{2.12}$$

$$k_0' = \frac{k_0 - E^*}{1 + \frac{2k_0}{M_T}\sin^2\frac{\theta}{2}} \approx k_0 - E^*. \tag{2.13}$$

Here E^* is the nucleus excitation energy (difference between the energies of the final and initial level); M_f -- nucleus mass. Summation in (2.12) is designated by Σ_f, and designates summation by pairs j_i and j_f.

Let us consider the simplest particular case, when the nucleus has filled l-shells (doubly magic) and we disregard the spin-orbital connection. Under these conditions, the expression similar to (2.9) for transition from the shells l_i in l_f has the following simple form:

$$\sum_{m_i m_f} \left\{ \eta_{\mu\nu} J_\mu J_\nu^* \right\} = 16 k_0 k_0' (2l_i+1)(2l_f+1) \sum_J \left\{ \left[\langle l_i 0\, l_f 0 | J 0 \rangle \right]^2 \cdot \right.$$

$$\left[\left(F_A^2 + F_1'^2 \frac{q^{*2}}{4M^2}\right)\left(\frac{q^2}{q^{*2}}\cos^2\frac{\theta}{2} + 2\sin^2\frac{\theta}{2}\right) + \left(\frac{q_0^2}{q^{*2}} + \frac{q_0}{M} + \frac{q^{*2}}{4M^2}\right) F_A^2 \cos^2\frac{\theta}{2} + \right. \tag{2.14}$$

$$\left. \left. + \frac{q^4}{q^{*4}} F_1^2 \cos^2\frac{\theta}{2} \mp \frac{2\sin\frac{\theta}{2}}{M} F_1' F_A \left(q^{*2}\sin^2\frac{\theta}{2} + q^2\cos^2\frac{\theta}{2}\right)^{1/2} \right] \cdot R^2_{n_f l_f J n_i l_i} \right\},$$

$$R_{n_f l_f J n_i l_i} \equiv \int_0^\infty R_{n_f l_f}(x)\, j_J(q^* x)\, R_{n_i l_i}(x)\, x^2 dx. \tag{2.10a}$$ /13

b) Transition in continuous spectra

For these transitions, the integral (2.6) may be written in the form:

$$J_\mu(\vec{q}) = \int e^{-i\vec{q}\vec{x}}\, \psi^{-*}_{\rho s_f}\, \hat{J}_\mu\, \psi_{n_i \ell_i j_i M_i}\, d\vec{x}\ ; \tag{2.15}$$

$$\psi^{-}_{\rho s_f} = \sum_{\ell_f j} \left\{ \sum_{m m'} \langle \ell_f m' \tfrac{1}{2} \mu' | j M \rangle \langle \ell_f m \tfrac{1}{2} s_f | j M \rangle\, Y_{\ell_f m'}(\hat{\vec{x}})\, Y_{\ell_f m}(\hat{\vec{p}})\, \chi_{\frac{1}{2}\mu'} \right\} \psi^{-}_{\rho \ell_f j}(x)$$

Here $\psi^{-}_{\rho s_f}$ is the wave function of the continuous spectrum for a nucleon with the energy $p^2/2m$ and the spin projection S_f (we use the representation of the channel spin [15]); $\psi_{\rho \ell_f j}(x)$ -- the corresponding radial function; $\chi_{\frac{1}{2}\mu}$ -- the eigen function of the operator σ_z $\left(\chi_{\frac{1}{2}\frac{1}{2}} = \begin{pmatrix}1\\0\end{pmatrix},\ \chi_{\frac{1}{2}-\frac{1}{2}} = \begin{pmatrix}0\\1\end{pmatrix}\right)$. The calculation of $\eta_{\mu\nu} J_\mu J^*_\nu$ is carried out similarly to the case of transitions in a discrete spectrum:

$$\sum_{s_f} \left\{ \eta_{\mu\nu} J_\mu J^*_\nu \right\} d\Omega_{\hat{p}} = 16 k_0 k_0' (2j_i+1) \sum_{\ell_f j} \left\{ (2j+1) \sum_{J J'} \left\{ (-1)^{\frac{1}{2}(J-J')} \cdot \right.\right.$$

$$\cdot \left[\left(\frac{q^2}{q^{*2}} \cos^2\frac{\theta}{2} + 2\sin^2\frac{\theta}{2} \right) \left(F_A^2 + F_1'^2 \frac{q^{*2}}{4M^2} \right) A^1_{J J' j_i j} + \cos^2\frac{\theta}{2} F_1^2 \frac{q^4}{q^{*4}} B_{J J' j_i j} + \right.$$

$$+ \cos^2\frac{\theta}{2} F_A^2 \left(\frac{q_0^2}{q^{*2}} + \frac{q_0}{M} + \frac{q^{*2}}{4M^2} \right) A^0_{J J' j_i j} \mp$$

$$\left. \left. \mp \frac{2\sin\frac{\theta}{2}}{M} F_1' F_A \left(q^{*2}\sin^2\frac{\theta}{2} + q^2\cos^2\frac{\theta}{2} \right)^{1/2} A^1_{J J' j_i j} \right] \cdot \right.$$

$$\left. \cdot R_{\rho \ell_f j J n_i \ell_i j_i} \cdot R_{\rho \ell_f j J' n_i \ell_i j_i} \right\} \right\}. \tag{2.16}$$

As previously, the functions $A^{1,0}$ and B are determined by the formulas (2.11), and the radial integrals now depend on the impulse $|\vec{p}|$, /14

$$R_{p\ell_f j_f n_i \ell_i j_i} \equiv \int \psi^{-}_{p\ell_f j}(x) j_J(q^* x) R_{n_i \ell_i j_i}(x). \qquad (2.17)$$

(2.16) includes summation over the projection of the spin of the channel S_f and over the direction of the nucleon flight. Therefore, we must integrate only with respect to the modulus $\vec{p}$. According to (2.1), the cross section equals:

$$\frac{d^2\sigma}{d\Omega\, dk_0'} = \frac{G^2}{2} \cdot \frac{1}{4k_0 k_0'} \cdot \frac{k'^2}{(2\pi)^3} \int 2\pi\, \delta(E_i - E_f + q_0) \left[\left\{ \left\{ \sum_{s_f} \eta_{\mu\nu} J_\mu \right\} J_\nu^* \right\} d\Omega_{\vec{p}} \right] \frac{p^2 dp}{(2\pi)^3}. \qquad (2.18)$$

Describing the cross sections of this form, we assume that the flight direction of the lepton and nucleon are independent, i.e., we disregard the limitations on the final state which arise due to the law of conservation of momentum. Strictly speaking, we would have to expand the wave functions of nucleons in the nucleus with respect to plane waves and to introduce the law of conservation of momentum explicitly into the calculation, which would greatly complicate the discussion. Up to a certain degree, we can compensate for this defect, by introducing a term considering the response into the energy δ-function, and assuming that this response is perceived by a free particle of the mass M^* (effective mass of the target):

$$\delta(E_i - E_f + q_0) = \delta\left(k_0 - k_0' + M_i - M_f - M - \frac{p^2}{2M} - E^* - \frac{q^2}{2M^*}\right). \qquad (2.19)$$

Here M_i and M_f are the masses of the initial and final (produced after the flight of the nucleon) nuclei; E^* -- excitation energy of the final nucleus. We obtain the following expression for the cross section:

$$\frac{d^2\sigma}{d\Omega\, dk_0'} = \frac{G^2}{(2\pi)^5} \cdot \frac{k_0'^2}{8k_0 k_0'} pM \left\{ \left\{ \sum_{s_f} \eta_{\mu\nu} J_\mu \right\} J_\nu^* \right\} d\Omega_{\vec{p}}, \qquad (2.20)$$

/15

and the connection of p with k_0' and the scattering angle is found

from the condition that the argument of the δ-function equal zero (2.19).

If we disregard the spin-orbital connection in the wave functions of the continuous spectrum, then (2.15) is reduced to the expression

$$\Psi^{-}_{\rho s_f} = \sum_{l_f m_f} \Psi^{-}_{\rho l_f}(x)\, Y_{l_f m_f}(\hat{\vec{x}})\, Y_{l_f m_f}(\hat{\vec{p}})\, \chi_{\frac{1}{2} s_f}, \qquad (2.21)$$

and formula (2.16) is greatly simplified:

$$\left\langle \left\{ \sum_{s_f} \eta_{\mu'} J_\mu J^{*}_{\mu'} \right\} d\Omega_{\vec{p}} \right\rangle = 16 k_0 k_0' (2j_i+1) \sum_{l_f} \left\{ (2l_f+1) \sum_{J} \left\{ \left[\langle l_i 0\, l_f 0 | J 0 \rangle \right]^2 \cdot \right.\right.$$

$$\cdot \left[\left(F_A^2 + F_1'^2 \frac{q^{*2}}{4M^2} \right) \left(\frac{q^2}{q^{*2}} \cos^2\frac{\theta}{2} + 2\sin^2\frac{\theta}{2} \right) + \left(\frac{q_0^2}{q^{*2}} + \frac{q_0}{M} + \frac{q^{*2}}{4M^2} \right) F_A^2 \cos^2\frac{\theta}{2} + \right.$$

$$\left.\left. + \frac{q^4}{q^{*4}} F_1^2 \cos^2\frac{\theta}{2} \mp \frac{2\sin\frac{\theta}{2}}{M} F_1' F_A \left(q^{*2}\sin^2\frac{\theta}{2} + q^2 \cos^2\frac{\theta}{2} \right)^{1/2} \right] R^2_{\rho l_f J n_i l_i j_i} \right\} \right\} \qquad (2.22)$$

2. Neutral current

a) Elastic scattering of neutrinos by a nucleus

This process, which occurs without excitation of the nucleus, is only possible due to a neutral current. Within the framework of the single particle shell model (single-determinant wave function of the nucleus) for the vector $J_\mu(\vec{q})$, we have the following expression, instead of (2.6),

$$J_\mu(\vec{q}) = \sum_j \psi_j(\vec{x})\, e^{-i\vec{q}\vec{x}}\, \hat{J}_\mu\, \psi_j(\vec{x})\, d\vec{x}, \qquad (2.23)$$

where ψ_j are the single particle wave functions, and summation is performed over all nucleons of the nucleus. We shall assume that the nuclear operator of the current $\hat{J}_\mu(\vec{x})$ is a mixture of an isoscalar and the third component of the isovector. For example, /16

for $\hat{J}_0(\vec{x})$, we have the following, instead of (2.4):

$$\hat{J}_0(\vec{x}) = \sum_i \Big\{ \left(F_1^0 + F_1^1\tau_3\right)\delta(\vec{x}-\vec{x}_i) + \left(F_A^0 + F_A^1\tau_3\right)\vec{\sigma}_i \cdot \cdot \left(\frac{\hat{\vec{p}}_i}{2M}\,\delta(\vec{x}-\vec{x}_i) + \delta(\vec{x}-\vec{x}_i)\,\frac{\hat{\vec{p}}_i}{2M} \right) \Big\} \qquad (2.24)$$

and similarly for $\hat{\vec{J}}(\vec{x})$. Substituting $\hat{J}_\mu(\vec{x})$ in (2.3), we obtain $J_\mu(\vec{q})$, which will have the form (2.23) with the following operator $\hat{J}_\mu$ [compare with (2.7)]:

$$\hat{\vec{J}} = -\left(F_1^0 + F_1^1\tau_3\right)\frac{\vec{q}}{2M} - i\left(F_1'^0 + F_1'^1\tau_3\right)\frac{\vec{\sigma}\times\vec{q}}{2M} + \left(F_A^0 + F_A^1\tau_3\right)\vec{\sigma} ,$$

$$\hat{J}_0 = \left(F_1^0 + F_1^1\tau_3\right) - \left(F_A^0 + F_A^1\tau_3\right)\frac{\vec{\sigma}\vec{q}}{2M} . \qquad (2.25)$$

Calculations, similar to those carried out above for the case of a charged current, lead to the following formula for the cross section of the elastic scattering of the neutrino by the nucleus:

$$\frac{d\sigma}{d\Omega} = \frac{G^2}{(2\pi)^2}\cdot\frac{1}{8k_0k_0'}\cdot\frac{k_0'^2}{1+\frac{2k_0}{M_T}\sin^2\frac{\theta}{2}}\,\eta_{\mu\nu}J_\mu J_\nu^* , \qquad (2.26)$$

$$\eta_{\mu\nu}J_\mu J_\nu^* = 16\,k_0k_0'\cos^2\frac{\theta}{2}\sum_{i,m}\sum_{j,j'}\Big\{(-1)^{\frac{1}{2}(j-j')}\Big[F_{1i}F_{1m}\frac{q^4}{q^{*4}}B_{jj'j_ij_m} + F_{Ai}F_{Am}\left(\frac{q_0^2}{q^{*2}}+\frac{q_0}{M}+\frac{q^{*2}}{4M^2}\right)A_{jj'j_ij_m}\Big]R_{ij}R_{mj'}\Big\} \qquad (2.27)$$

Here we use the notation:

$$R_{ij} \equiv \int R_{n_i l_i j_i} j_J(q^* x) R_{n_m l_m j_m} x^2 dx ,$$

$$A_{JJ' j_i j_m} \equiv (-1)^{j_i + j_m + 1} \sqrt{(2j_i+1)(2j_m+1)} \cdot \sum_{M_i M_m} \sum_{cc'} \left\{ \sqrt{(2c+1)(2c'+1)} \cdot \right.$$

$$\langle j_i M_i c 0 | j_i M_i \rangle \langle j_m M_m c' 0 | j_m M_m \rangle \langle J 0 1 0 | c 0 \rangle \langle J' 0 1 0 | c' 0 \rangle \cdot$$

$$\left. \cdot \langle j_i \tfrac{1}{2} j_i - \tfrac{1}{2} | c 0 \rangle \langle j_m \tfrac{1}{2} j_m - \tfrac{1}{2} | c' 0 \rangle f(Jc) f(J'c) \right\} ,$$

$$B_{JJ' j_i j_m} \equiv (-1)^{j_i + j_m + 1} \sqrt{(2j_i+1)(2j_m+1)(2J+1)(2J'+1)} \cdot \qquad (2.28)$$

$$\cdot \sum_{M_i M_m} \left\{ \langle j_i M_i J 0 | j_i M_i \rangle \langle j_m M_m J' 0 | j_m M_m \rangle \langle j_i \tfrac{1}{2} j_i - \tfrac{1}{2} | J 0 \rangle \langle j_m \tfrac{1}{2} j_m - \tfrac{1}{2} | J' 0 \rangle \right\} .$$

Summation is performed in (2.27) over all pairs of nucleons in the nucleus (including i = m). The form factors F_{1i} and F_{Ai} in (2.27) have the following meaning: if i is a proton, then $F_{1,Ai} = F_{1,A}^{0} + F_{1,A}^{1}$; if i is a neutron, then $F_{1,Ai} = F_{1,A}^{0} - F_{1,A}^{1}$

Formula (2.26) generalizes the expressions in the literature [16] to the region of average energies. For small ($E_f \sim$ 20 MeV) energies ("astrophysical" energy region), in (2.27) we may confine ourselves to terms with $J = J' = 0$. In this case

$$B_{00 j_i j_m} = (2j_i+1)(2j_m+1) , \quad A_{00 j_i j_m} = 0 ,$$

$$\eta_{\rho\gamma} \frac{d\sigma}{d\Omega}\Big|_0^{\pi} \approx 16 k_0 k_0' \cos^2 \frac{\theta}{2} \cdot \left[F_1^0 A + F_1^1 (Z-N) \right]^2 . \qquad (2.29)$$

It may be seen from (2.29) that the isoscalar part of the stream leads to the coherent cross section ($A = Z + N$): /18

$$\left(\frac{d\sigma}{d\Omega}\right)_{coh.} \approx \frac{G^2}{2\pi^2} k_0'^2 \cos^2\frac{\theta}{2} \left(F_1^0\right)^2 A^2. \qquad (2.30)$$

In particular, $F_1^0 = -\sin^2\theta_W$. 2in the Weinberg-Salam model [17].

b) Inelastic scattering (excitation of the nucleus)

A separate calculation is not required here, since it is completely similar to the case of the charged stream. The only change consists of the fact that now the cross section is divided into two parts -- the proton (p-p transitions) and the neutron (n-n transitions). Each part, for a corresponding replacement of the form factors, may be calculated according to the formulas given above.

3. Calculation results

In deriving the formulas for the cross sections, it was assumed above that the nucleus-target has completely filled j-shells, and, consequently, there are unideterminant wave functions in our model. In order to approximately consider the real filling of the shells with nucleons, each single particle cross section describing the transition between two shells is multiplied by the coefficient [18]:

$$\alpha = \frac{N_i}{2j_i+1} \cdot \frac{N_f}{2j_f+1}$$

Here N_i is the number of occupied positions in the j_i-shell, and N_f is the number of free positions in the j_f-shell. In this case of discrete-continuous transitions with j_i-shells, the corresponding single particle cross section is multiplied by

$$\beta = \frac{N_i}{2j_i+1}.$$

All of the form factors of weak interaction for nucleons in the nuclei were selected just the same as for free nucleons. In /19

the case of a charged stream, using the hypothesis of conservation of the vector stream [19], we identified the weak vector form factors F_1 and F_2 of the nucleon with the isovector electromagnetic Dirac and Pauli form factors:

$$F_{1,2}(q^2) = F_{1,2}^{p}(q^2) - F_{1,2}^{n}(q^2) . \qquad (3.1)$$

Thus $F_1(0) = 1$, $2MF_2(0) = \mu_p - \mu_n \approx 3{,}706$. Here, $\mu_p = 1.79$, $\mu_n = -1.91$ -- anomalous magnetic moments of the proton and neutron. For $F_A(0)$, we use the value -1.24 [20]. The dependence of the form factors on q^2 may be described by the dipole formula

$$F_i(q^2) = F_i(0) \cdot \left(1 + \frac{q^2}{M_1^2}\right)^{-2}, \quad i = 1,2,A . \qquad (3.2)$$

$F_1' = F_1 + 2MF_2$.

Here $M_1 = 840$ MeV [21]. In the case of a neutral stream, we represent the form factors in the form of the sum of the isoscalar and isovector parts:

$$F_i(q^2) = F_i^{0}(q^2) + F_i^{1}(q^2)\tau_3 . \qquad (3.3)$$

Here the index 0 corresponds to the isoscalar part, and the index 1 -- to the isovector part of the stream. In the Weinberg-Salam model

$$\begin{aligned} &F_1^{0}(0) = -\sin^2\theta_w , \quad F_1^{1}(0) = \tfrac{1}{2}\left(1 - 2\sin^2\theta_w\right) , \\ &2MF_2^{0}(0) = -\sin^2\theta_w \cdot (\mu_p + \mu_n) , \quad 2MF_2^{1}(0) = \tfrac{1}{2}\left(1 - 2\sin^2\theta_w\right)(\mu_p - \mu_n) , \\ &F_A^{0}(0) = 0 , \quad F_A^{1}(0) = \tfrac{1}{2} F_A(0) . \end{aligned} \qquad (3.4)$$

For the Weinberg angle θ_w, we use $\sin^2\theta_w = 0.3$. Then we have the following for the transitions between the proton states:

$$F_{1p} = \tfrac{1}{2}\left(1 - 4\sin^2\theta_w\right) = -0{,}1 ,$$

$$F_{1p}^{0}(0) = F_{1p}(0) + 2MF_{2p}(0) = -0{,}1 - \sin^2\theta_w (\mu_p + \mu_n) +$$

$$+\frac{1}{2}\left(1-2\sin^2\theta_w\right)\left(\mu_p-\mu_n\right)=0{,}676\,,$$

$$F_{Ap}(0)=\frac{1}{2}F_A(0)=-0{,}62.$$

For transitions between the neutron states

$$F_{1n}(0)=-0{,}5,$$

$$F'_{1n}(0)=-0{,}5-\sin^2\theta_w\left(\mu_p+\mu_n\right)-\frac{1}{2}\left(1-2\sin^2\theta_w\right)\left(\mu_p-\mu_n\right)=-1{,}204,$$

$$F_{An}(0)=-\frac{1}{2}F_A(0)=0{,}62.$$

For calculations of the inelastic process cross sections (1.1), (1.2), we have written a program making it possible to calculate the wave functions of the discrete and continuous spectra and the eigen energies of the connected states using the given nuclear potential. We can also calculate the cross sections of the processes examined using the formulas given in section 2. Appendix C gives greater details about the selection of the nuclear potential and the numerical calculations of the wave functions and the interaction cross sections. In the calculations of the discrete-continuous transitions, we have assumed an effective mass of the target which equals the nucleon mass.

For specific numerical calculations, we selected the following nuclei ^{12}C, ^{16}O, ^{37}Cl ^{56}Fe, ^{71}Ga, ^{81}Br. The neutrino reactions with the nuclei are important both for accelerating experiments (with the ^{12}C, ^{16}O, ^{56}Fe nuclei), and for experiments with solar neutrinos (^{37}Cl, ^{71}Ga, ^{81}Br). The neutrino interaction cross sections with detector nuclei (such as ^{37}Cl, ^{71}Ga, ^{81}Br) must be known in a wide range of the energy changes E_ν (0-1 GeV) in order to evaluate the background of the cosmic ray neutrinos in the experiments [5]

(the background arises from the interaction of the cosmic ray neutrinos with the detector nuclei). On the basis of the formulas obtained for the cross sections and the program, we can estimate the background for an arbitrary detector. /21

In addition, for reactions of neutrinos with the nuclei examined, other authors have made calculations, whose results can be compared with ours [1-8].

As a result of the calculations, we obtain differential and complete cross sections of inelastic reactions (1.1) and (1.2) occurring due to charged (n-p-transitions) and neutral streams (p-p and n-n-transitions). Figures 1-12 give the basic computational results.

Below, for brevity, we shall designate the discrete-discrete transitions as g-g, and discrete-continuous transitions as g-н .

Figures 1-6 show the cross section $\sigma(E_\nu)$ of the reactions (1.1) and (1.2) using the formulas given in the second paragraph, for the nuclei ^{12}C, ^{16}O, ^{37}Cl, ^{56}Fe, ^{71}Ga, ^{81}Br. The solid lines show the behavior of the sum of the cross sections $\sigma_{gg+gн}$ $_{gg}$ and $_{gн}$ of the transition; the dashed lines show the individual cross sections σ_{gg} $_{gg}$ of the transition. The numbers 1, 2, 3 designate the transitions caused by a charged stream (n-p) and the transitions due to neutral streams (n-n) and p-p). The behavior of the cross sections of the reaction (1.2) is similar to the behavior of the cross section for the reaction with charged streams (1.1), since the difference in these cross sections is basically due to a difference in the form factors. The total cross section of the n-n and p-p transitions is approximately 30% of the cross section of the reaction (1.1) almost in the entire region of the change in E , except for the region $E_\nu < 40$ MeV, which is close to the threshold of the reactions examined.

Figure 7 gives the total cross section $\sigma_{gg+gн}$ of the reaction (1.1) for the nucleus ^{16}O with closed n and p shells, along /22

with the results obtained by other authors. In the $E_\nu < 80$ MeV energy region, which is close to the threshold, where the cross section of the g^H transition is much less than the cross section of the gg transitions, the cross section we obtained is similar to the total cross section of the transitions between all individual levels examined in [3], obtained by adjusting the experimental data. In the $E_\nu > 80$ MeV region, the cross section of the g^H transitions predominates; therefore, our cross section is greater than the total cross section obtained in [3]. The shell calculations performed using the approximation of completeness [8] in the $E_\nu < 200$ MeV region, lead to a larger value of the cross section than with ours, and at $E_\nu = 300$ MeV it is approximately 2 times smaller than ours. It is known that the study [8] could not explain the experimental behavior of the cross section 12 obtained at Argonne [22] (the theoretical values were less than the experimental values by a factor of approximately 2-3 at q^2 0.05 GeV^2). The results of our study show that this divergence may be reduced, if we consider the transitions more exactly in the continuous spectrum state. At $E_\nu = 300$ MeV our cross section approximates the cross section of the reaction (1.1) for 8 free neutrons.

Figures 1, 3, 4, 7 use the crosses to designate the cross section for the reaction (1.1) obtained in the Fermi-gas model in [7], where the matrix elements were taken from experimental data with respect to the μ-capture. For light nuclei (^{12}C, ^{16}O), the method used in [7] is worse than for average and heavy nuclei, and the agreement with our shell calculations is not good enough, whereas for ^{37}Cl and ^{56}Fe cross sections, which we obtained within the framework of the shell model and the Fermi-gas model, coincide in the examined region of neutrino energy. The cross section formulated from the ^{16}O on the basis of the Fermi-gas calculations from [12] behaved similarly to the cross section from [7]. /23

Figure 8 shows the total cross section $\sigma_{gg \to g^H}$ for ^{12}C [the reaction (1.1)] and the cross section obtained for the same reaction in [1]. The divergence between our cross section and the

cross section from [1] is great for small E_ν, in contrast to the cross section of the reaction with ^{16}O, which is apparently related to the fact that the ^{12}C is a light nucleus having a cluster structure to which our shell model is only slightly applicable.

Figure 9 makes a comparison of the total cross section for one neutron for the reaction (1.1) for all of the nuclei examined, with the cross section of the reaction (1.1) for a free nucleon, given in [12]. It may be seen that the difference in the cross section $\sigma(E_\nu)/N$ is great at $E_\nu < 100$ MeV. For large energies the differences become small, and at $E_\nu \approx 300$ MeV the cross sections approximate a single-nucleon cross section.

Figure 10 makes a comparison of the cross sections $d\sigma/d\Omega$ of the reaction (1.1) obtained in different models for the case ^{16}O at $E_\nu = 300$ MeV.

Figure 11 gives the reduced differential cross sections $(d\sigma/d\Omega)/N$ for all of the nuclei examined and makes a comparison with the cross section $d\sigma/d\Omega$ for a free nucleon. In connection with these figures, we should note the following. In the low angle region (for fixed energy E_ν of the corresponding region of small q^2), the experiment gives much larger cross sections than theory. As was noted in the study of Cannata and Leonardi [13], in this region it is necessary to consider relativistic terms in the expansion of the nucleon stream, and also to consider the collective effects in the nucleus.

Figure 12 shows the quasi-elastic peaks $d^2\sigma/d\Omega\, dE_e$ for the reactions (1.1) in the nucleus ^{16}O, calculated on the basis of our model and the Fermi-gas model [12]. The difference in the positions /24 of the quasi-elastic peaks in these models is due to the fact that there are no thresholds in the Fermi-gas model for the reactions (1.1) and (1.2), and the nucleons do not occur in the potential hole.

4. Conclusion

We have described the processes of inelastic and elastic neutrino-nuclear reactions in a wide range E within the framework of a single-particle shell model of the nucleus with the Woods-Saxon potential. This description represents a step forward as compared with the simple model of the Fermi-gas, since the use of the potential with a finite depth makes it possible to describe the state of the continuum and the related states using the solution of the Schroedinger equation with this potential. The parameters of the potential were determined so that the energies obtained of the connected states and the thresholds of the single-particle transitions were similar to the experimental values. We calculated the sums of all possible transitions in the connected excited states and in the state of the continuum for nuclei of ^{12}C, ^{16}O, ^{37}Cl, ^{56}Fe, ^{71}Ga, ^{81}Br in the neutrino energy range of $0 \leq E_\nu \leq 300$ MeV. An examination was made of reactions taking place due to the charged streams and due to neutral streams of weak interaction. It is shown that the cross sections of inelastic reactions occurring due to the neutral streams represent approximately 30% of the value for the cross section of reactions with charged streams.

The method described in this article is universal, and may be applied to any nuclei, and gives good accuracy for nuclei with closed shells. Only the parameters of the Wood-Saxon potential are necessary, which lead to a system of levels of the nucleus which is close to the experimental one.

In calculations of transitions in a continuous spectrum, we disregarded the possibility of a nucleon sticking in the nucleus, and it was assumed that the potential is real. For small q, the probability of a nucleon sticking in the nucleus is great. With an increase in q, the probability of a direct flight of a nucleon participating in the reaction increases. For a more exact representation of the state of the final nucleus, calculations are necessary which consider the imaginary part of the optical potential, and

/25

also the calculation of the evaporation processes of nucleons from the excited nuclei. In the high energy region, the results obtained using the shell model are similar to the results obtained using the Fermi-gas model. The situation is more complex in the threshold energy range, since there it is necessary to consider the residual interaction of nucleons in the nucleus. Not considering this fact leads to the fact that the cross section we obtain exceeds the real one by approximately a factor of two for nuclei with unfilled shells of the ^{12}C type, as would be expected from comparing our cross sections with cross sections obtained using a careful adjustment of the experimental data [1],[3].

It is also necessary to consider the residual interaction in order to find a more exact distribution of the energy probabilities for the excitation of the final nucleus.

APPENDIX A

/26

Let us give the basic stages in deriving the formula (2.5) for the convolution of $\eta_{\mu\nu} J_\mu J_\nu^*$. First of all, by direct calculation using (2.2) we obtain the expression

$$\eta_{\mu\nu} J_\mu J_\nu^* = 8 k_0 k_0' \left\{ 2\,\mathrm{Re}\left[\left(\frac{\vec{k}}{k_0} \vec{J} \right)\left(\frac{\vec{k}'}{k_0'} \vec{J}^* \right) - \left(\frac{\vec{k}'}{k_0'} + \frac{\vec{k}}{k_0} \right) J_0 \vec{J}^* \right] + \right.$$

$$+ |J_0|^2 \frac{1}{2}\left(1 + \frac{\vec{k}\vec{k}'}{k_0 k_0'} \right) + |\vec{J}|^2 \frac{1}{2}\left(1 - \frac{\vec{k}\vec{k}'}{k_0 k_0'} \right) \mp \tag{A.1}$$

$$\left. \mp \mathrm{Im}\left[2 J_0^* \vec{J} \frac{[\vec{k}\vec{k}']}{k_0 k_0'} + \left(\frac{\vec{k}}{k_0} - \frac{\vec{k}'}{k_0'} \right)[\vec{J}\vec{J}^*] \right] \right\}.$$

It is more convenient to use the fact that (see [23]) the cross section in which we are interested is summed over all spins and integrated with respect to the flight angles of all particles (except for a lepton). The unique vector, which "exists" after the summation, is the vector q. Therefore, all three-dimensional vectors and tensors (not lepton) existing in (A.1) may be expressed (after summation) by the components of the vector q and the tensor $\delta_{\alpha\beta}$ and $q_\alpha q_\beta$ ($\alpha, \beta = 1, 2, 3$). Consequently, we may write (the bar above indicates the summation):

$$\overline{J_0 \vec{J}^*} = \bar{A} \vec{q}\,, \quad A = \frac{1}{\vec{q}^2} \overline{J_0 (\vec{J}^* \vec{q})}\,; \tag{A.2}$$

$$\overline{J_\alpha J_\beta^*} = \bar{B} \delta_{\alpha\beta} + \bar{C} q_\alpha q_\beta\,, \quad \bar{B} = \frac{1}{2}\overline{|\vec{J}|^2} - \frac{1}{2\vec{q}^2}\overline{(\vec{q}\vec{J})(\vec{q}\vec{J}^*)}\,,$$

$$\bar{C} = \frac{3}{2q^4}\overline{(\vec{q}\vec{J})(\vec{q}\vec{J}^*)} - \frac{1}{2\vec{q}^2}\overline{|\vec{J}|^2}\,; \tag{A.3}$$

$$\overline{[\vec{J}\vec{J}^*]} = \bar{D}\vec{q}\,, \quad \bar{D} = \frac{1}{\vec{q}^2}\vec{q}\,\overline{[\vec{J}\vec{J}^*]}. \tag{A.4}$$

/27

It follows from (A.2) - (A.4) that we may make the following substitution directly before the summation, i.e., in (A.1):

$$J_\perp \to \frac{1}{\vec{q}^2}(\vec{J}\vec{q})q_\perp \ , \quad [\vec{J}\vec{J}^*]_\perp \to Dq_\perp \ ,$$
$$J_\perp J_\beta^* \to B\delta_{\perp\beta} + C q_\perp q_\beta \ , \tag{A.5}$$

(the functions B, C and D are found from (A.3) - (A.4) by removing the bar above).

We selected the coordinate system so that the vector $\vec{q}$ is distributed along the Z-axis. Except for $\vec{q}$, we have two lepton vectors:

$$\frac{\vec{k}}{k_0} \equiv \vec{n} \ , \quad \frac{\vec{k}'}{k_0'} \equiv \vec{n}' \ , \quad \vec{n}\vec{n}' = \cos\theta \ . \tag{A.6}$$

The first and second terms in (A.1) may be transformed considering (A.5) as follows:

$$(\vec{n}\vec{J})(\vec{n}'\vec{J}^*) \to |J_z|^2\cos\theta - \frac{3}{2}|J_z|^2\frac{q_\nu^2}{q^{*2}}\cos^2\frac{\theta}{2} + \frac{1}{2}|\vec{J}|^2\frac{q_\nu^2}{q^{*2}}\cos^2\frac{\theta}{2} \ ,$$
$$(\vec{n}+\vec{n}')J_0\vec{J}^* \to 2\frac{q_0}{q^*}J_0J_z^*\cos^2\frac{\theta}{2} \ . \tag{A.7}$$

The first component in the last term in (A.1) may be discarded, since

$$2J_0\vec{J}^*\frac{[\vec{k}\vec{k}']}{k_0k_0'} \to 2J_0J_z^*\frac{[\vec{k}\vec{k}']\vec{q}}{k_0k_0'q^*} = 0$$

(we recall that $\vec{q} = \vec{k} - \vec{k}'$).

Finally, we transform the last component in (A.1):

$$(\vec{n}-\vec{n}')[\vec{J}\vec{J}^*] \to -\frac{2\sin\frac{\theta}{2}}{q^4}\left(q_0^2\sin^2\frac{\theta}{2} + q_\nu^2\cos^2\frac{\theta}{2}\right)^{1/2}(J_xJ_y^* - J_yJ_x^*) \ . \tag{A.8}$$

/28

Collecting all the formulas, we reach the expression (2.5) for $n_{\mu\nu}\,\mathcal{J}_{\mu}\,\mathcal{J}_{\nu}^{*}$.

APPENDIX B

We shall explain in general features how we derived the formulas (2.9), (2.16) and (2.27). We first perform summation over the spins and perform integration with respect to the angles in the integrals (2.6). Expanding the exponent in this integral in series in terms of spherical functions,

$$e^{-i\vec{q}\vec{x}} = \sum_{J=0}^{\infty} \sqrt{4\pi(2J+1)}\,(-i)^{J}\, j_J(q^{*}x)\, Y_{J0}\left(\hat{\vec{x}}\right), \tag{B.1}$$

we reduce this problem to calculating the following two standard integrals:

$$\left\langle \ell_f j_f M_f \left| \frac{\sigma_\mu}{2} Y_{J0} \right| \ell_i j_i M_i \right\rangle = \sqrt{\frac{3}{8\pi}} \cdot \sqrt{(2j_i+1)(2\ell_i+1)(2J+1)} \cdot \langle \ell_i 0\, J0 | \ell_f 0\rangle \cdot$$

$$\cdot \sum_c \sqrt{2c+1}\, \langle j_i M_i\, cK | j_f M_f\rangle \langle J0\, 1K | cK\rangle \begin{Bmatrix} \ell_i & J & \ell_f \\ \frac{1}{2} & 1 & \frac{1}{2} \\ j_i & c & j_f \end{Bmatrix},$$

$$\left\langle \ell_f j_f M_f | Y_{J0} | \ell_i j_i M_i \right\rangle = \sqrt{\frac{1}{4\pi}} \cdot \sqrt{(2j_i+1)(2\ell_i+1)(2J+1)} \cdot \tag{B.2}$$

$$\cdot \langle \ell_i 0\, J0 | \ell_f 0\rangle \langle j_i M_i\, J0 | j_f M_f\rangle \cdot \begin{Bmatrix} \ell_i & \frac{1}{2} & j_i \\ j_f & J & \ell_f \end{Bmatrix} \cdot (-1)^{j_i+\ell_f+J+\frac{1}{2}}.$$

We also use the following formulas for $9j$ and $6j$ symbols [24]:

$$\sqrt{(2\ell_i+1)(2J+1)}\,\langle \ell_i 0\, J 0|\ell_f 0\rangle \begin{Bmatrix} \ell_i & J & \ell_f \\ \frac{1}{2} & 1 & \frac{1}{2} \\ j_i & C & j_f \end{Bmatrix} =$$

$$= (-1)^{j_f + C - \frac{1}{2}} \frac{f(JC)}{\sqrt{6(2J+1)}} \langle j_i \tfrac{1}{2}\, j_f -\tfrac{1}{2}|C0\rangle , \qquad (B.3)$$

$$\sqrt{(2\ell_i+1)(2J+1)}\,\langle \ell_i 0\, J 0|\ell_f 0\rangle \begin{Bmatrix} \ell_i & \frac{1}{2} & j_i \\ j_f & J & \ell_f \end{Bmatrix} = (-1)^{j_i + j_f + \ell_f} \langle j_i \tfrac{1}{2}\, j_f -\tfrac{1}{2}|C0\rangle .$$

The function $f(JC)$ is determined by the formulas:

$$f(CC) = \frac{x_i - x_f}{\sqrt{C(C+1)}} ,$$

$$f(C-1,C) = \frac{1}{2C+1}\sqrt{\frac{2C-1}{C}}\,(x_i + x_f - C) ,$$

$$f(C+1,C) = \frac{1}{2C+1}\sqrt{\frac{2C+3}{C+1}}\,(x_i + x_f + C + 1) , \qquad (B.4)$$

$$x_{i,f} = (2j_{i,f}+1)(\ell_{i,f} - j_{i,f}) .$$

Substituting (B.3) into (B.2), we obtain simple expressions for our integrals:

$$\langle \ell_f j_f M_f | \frac{\sigma_K}{2} Y_{J0} | \ell_i j_i M_i \rangle = \frac{(-1)^{j_f + C - \frac{1}{2}}}{2\sqrt{4\pi(2J+1)}} \sqrt{2j_i+1} \cdot$$

$$\cdot \sum_C \left\{ \sqrt{2C+1}\,\langle j_i M_i CK | j_f M_f\rangle \langle J0\,1K|CK\rangle \langle j_i \tfrac{1}{2}\, j_f -\tfrac{1}{2}|C0\rangle f(JC) \right\} , \qquad (B.5)$$

$$\langle \ell_f j_f M_f | Y_{J0} | \ell_i j_i M_i \rangle = (-1)^{j_f + J - \frac{1}{2}} \sqrt{\frac{2j_i+1}{4\pi}}\,\langle j_i M_i J0 | j_f M_f\rangle \langle j_i \tfrac{1}{2}\, j_f -\tfrac{1}{2}|J0\rangle .$$

The Klebb-Jordan coefficients, containing $j_i M_i$ and $j_f M_f$ are lost during squaring and summation over M_i and M_f, /30

$$\sum_{M_i M_f} \langle j_i M_i c K | j_f M_f \rangle \langle j_i M_i c' K' | j_f M_f \rangle = \frac{2j_f+1}{2c+1} \delta_{cc'} \delta_{KK'}.$$

For example, we obtain the following result for the term in (2.5), which is proportional to $|J_2|^2$

$$\sum_{J,J'} \sum_{M_i M_f} 4\pi \sqrt{(2J+1)(2J'+1)} \langle \psi_f | \left(F_1 \frac{q_0}{q^2} + F_A \sigma_0\right) Y_{J0} | \psi_i \rangle \langle \psi_f | \left(F_1 \frac{q_0}{q^2} + F_A \sigma_0\right) Y_{J'0} | \psi_i \rangle^* =$$

$$= (2j_i+1)(2j_f+1) \sum_{J,J'} \left\{ (-1)^{\frac{1}{2}(J-J')} \left\{ F_1 \frac{q_0^2}{q^2} \delta_{JJ'} \left[\langle j_i \tfrac{1}{2} j_f -\tfrac{1}{2} | J0 \rangle \right]^2 + \right. \right. \qquad \text{(B.6)}$$

$$\left. \left. + F_A^2 \sum_c \left[\langle J0\,10 | c0 \rangle \langle J'0\,10 | c0 \rangle \left[\langle j_i \tfrac{1}{2} j_f -\tfrac{1}{2} | c0 \rangle \right]^2 \right\} \right\}$$

The interferential terms, which are proportional to the product of the vector and axially-vector form factors, are reduced during summation over T and T' always, with the exception of the last component in (2.5).

We may readily obtain the formulas for the particular cases [(2.14) and (2.22)] not by using (B.3), but directly by using the following well-known relationships in (B.2) [25]:

$$\sum_c (-1)^{l_i + l_f + 1 + c} \sqrt{2(2l_f+1)(2j_i+1)(2c+1)} \langle 1K\,J0 | cK \rangle \langle j_i M_i cK | j_f M_f \rangle \cdot$$

$$\cdot \begin{Bmatrix} l_i & J & l_f \\ \frac{1}{2} & 1 & \frac{1}{2} \\ j_i & c & j_f \end{Bmatrix} = \sum_{m_{l_i}} \left\{ \langle l_i m_{l_i} \tfrac{1}{2} \tfrac{s_i}{2} | j_i M_i \rangle \langle l_f m_{l_f} \tfrac{1}{2} \tfrac{s_f}{2} | j_f M_f \rangle \langle \tfrac{1}{2} \tfrac{s_i}{2} 1K | \tfrac{1}{2} \tfrac{s_f}{2} \rangle \langle J0\, l_i m_{l_i} | l_f m_{l_f} \rangle \right\}, \qquad \text{(B.7)}$$

$$(-1)^{j_i + l_f + J + \frac{1}{2}} \sqrt{2j_i+1} \langle j_i M_i J0 | J_f M_f \rangle \begin{Bmatrix} l_i & \frac{1}{2} & j_i \\ j_f & J & l_f \end{Bmatrix} =$$

$$= \frac{1}{\sqrt{2l_f+1}} \sum_{m_{l_i}} \left\{ \langle l_i m_{l_i} \tfrac{1}{2} \tfrac{s_i}{2} | j_i M_i \rangle \langle l_f m_{l_f} \tfrac{1}{2} \tfrac{s_f}{2} | j_f M_f \rangle \langle l_i m_{l_i} J0 | l_f m_{l_f} \rangle \right\}$$

APPENDIX C

/31

Selection of Effective Nuclear Potential and Certain Details of Numerical Calculation

1. Discrete spectra

The wave functions and the eigen energies of the discrete spectrum were calculated by solving the Schroedinger equation with the effective nuclear potential in the Woods-Saxon form (considering the Coulomb potential for the protons). The potential was taken in the following form:

$$V(x) = V_c(x) - V_0 f_0(x) + V_s\left(\frac{\hbar}{m_\pi c}\right)^2 \cdot \frac{1}{x} \cdot \frac{df_s}{dx} \cdot 2\hat{\vec{l}}\hat{\vec{s}} \; ; \qquad (C.1)$$

$$f_i(x) = \left\{1 + \exp\left[(x - R_i)/a_i\right]\right\}^{-1} \quad , \; i = 0, s \; ;$$

$$2\hat{\vec{l}}\hat{\vec{s}} = \begin{cases} l & , \; j = l + 1/2 \\ -l-1 & , \; j = l - 1/2 \end{cases} . \qquad (C.2)$$

The Coulomb potential $V_c(X)$ was assumed to equal the potential of a uniformly charged sphere with the radius R_0 and the charge $(Z-1)e$

$$V_c(x) = (Z-1)\frac{e^2}{x^2}\zeta(x) , \qquad (C.3)$$

where, for the protons

$$\zeta_p(x) = \begin{cases} \frac{3}{2}\frac{x}{R_0} - \frac{1}{2}\left(\frac{x}{R_0}\right)^3 & \text{at } x \leq R_0 \\ 1 & \text{at } x > R_0 \end{cases} \qquad (C.4)$$

for the neutrons

$$\zeta_n(x) = 0 . \qquad (C.5)$$

To solve the Schroedinger equation, a program was written making it possible to find the wave functions and the eigen energies of all

the states of the discrete spectrum using the given A and Z. /32

For the ^{12}C and ^{16}O nuclei, we made several detailed calculations with different values of the parameters for the nuclear potential in order to obtain partial transitions in the reactions (1.1) and (1.2), which were similar to the experimental values for the thresholds. This was due to the fact that, as the calculations showed, the cross sections of the partial transition between two levels depend mainly on the difference between the eigen energies of these levels, i.e., on the threshold, and to a lesser extent, the asbsolute values of the energies of the levels. For ^{12}C, we finally selected the following set of the potential parameters (C.1) - (C.5):

$$V_{on} = V_{op} = 51 \text{ MeV} \quad V_{sn} = V_{sp} = 19{,}1 \text{ Mev}$$

$$a_{on} = a_{op} = 0{,}67 \text{ f} ; \; r_{on} = r_{op} = 1{,}27 \text{ f}. \tag{C.6}$$

The quantities R_o and R_s were calculated in the case ^{12}C using the formula

$$R_{o,s} = r_{o,s} A^{1/3} \tag{C.7}$$

For the nuclei ^{16}O, ^{37}Cl, ^{56}Fe, ^{71}Ga, ^{81}Br, the values of r_i, a_i and V_s for the potentials (C.1) - (C.2) were taken on the basis of the study [26]. These parameters are given in Table 1.

The values of the quantities V_{on} and V_{op} for ^{16}O are the following:

$$V_{on} = 56 \text{ MeV} \quad V_{op} = 52 \text{ MeV}. \tag{C.8}$$

For ^{37}Cl, ^{56}Fe, ^{71}Ga, ^{81}Br, we used the interpolation formulas from [27] for V_{on} and V_{op}:

$$V_{on} = 49{,}84 - 46{,}5 \cdot (N-Z)/A \quad \text{(MeV)}$$
$$V_{op} = 57{,}8 + 9{,}2 \cdot (N-Z)/A \quad \text{(MeV)} \tag{C.9}$$

The quantities R_0 and R_s for these five nuclei were determined using the formula [26]:

$$R_i = r_i (A-1)^{1/3}, \quad i = 0,s. \tag{C.10}$$

The potential (C.1) - (C.5) with parameters determined from (C.9) and (C.10) and Table 1 make it possible to obtain the energy of the upper filled single-particle levels, coinciding with the experimental data in a wide range of A and Z. Table 2 gives the values of single-particle energy levels for all of the nuclei which we examined, obtained as the result of numerical calculations. /33

The Schroedinger equation for the radial part of the wave function $R_{nlj}(x)$ of the nucleon, located in a field with the potential (C.1) - (C.5), was solved in the usual way [28] using the substitution of $y_{nlj}(x) = x R_{nlj}(x)$, as the result of which the following equation was obtained for $y_{nlj}(x)$

$$y''_{nlj}(x) - \frac{l(l+1)}{x^2} y_{nlj}(x) + 0,04823 \left[E_{nlj} + V_0 f_0(x) - 1,9968 V_s \frac{1}{x} \frac{df_s}{dx} \cdot \right.$$

$$\left. \cdot 2\hat{\vec{l}}\hat{\vec{s}} \right] y_{nlj}(x) - 0,06939 (Z-1) \cdot \frac{\zeta(x)}{x} y_{nlj}(x) = 0, \tag{C.11}$$

where $E_{nlj} < 0$ is the eigen energy of the level with the quantum numbers n, l, j.

The solution (C.1) must satisfy the boundary conditions $y_{nlj}(0) = y_{nlj}(\infty) = 0$ and the normalization condition $\int_0^\infty y^2 dx = 1$.

In a small region close to the center of a nucleus $0 < x \leq x_1 < R$ the solution is selected in the form of the spherical Bessel function

$$y_{nlj}(x) = N_1 j_l(\beta x), \tag{C.12}$$

where for the neutrons $\beta = [0{,}04823(V_0 + E_{nlj})]^{1/2}$, and for the protons $\beta = [0{,}04823(V_0 + E_{nlj}) - 0{,}10409(Z-1)/R]^{1/2}$. The quantity x_1 was selected to equal 0.4 f.

As the solution at $X \to \infty$, we selected the Whittaker function $W(-\eta, l+1/2, 2kx)$, where $K = (0{,}04823|E_{nlj}|)^{1/2}$, $\eta = 0{,}06939(Z-1)/2K$ /34
for protons and $\eta = 0$ for neutrons. Using its integral representation, we may write

$$y_{nlj}(x) = N_2 e^{-kx - \eta \ln 2kx} \int_0^\infty t^{l+\eta} \left(1 + \frac{t}{2kx}\right)^{l-\eta} e^{-t} dt . \qquad (C.13)$$

In the case of the neutrons $\eta = 0$ and the function W is reduced to the Hankel function of the imaginary argument, which can be represented in the form of the finite series:

$$y_{nlj}(x) = N_2' e^{-\rho} \left[1 + \frac{l(l+1)}{1!\,2\rho} + \frac{l(l-1)(l+1)(l+2)}{2!\,(2\rho)^2} + \dots\right], \qquad (C.14)$$

where $\rho = kx$. The quantities N_1, N_2, N_2' are arbitrary numerical factors.

In the case of protons, we obtain the function W and its derivative with respect to x, calculating the integral from (C.13) and the integral of a similar type arising in the calculation of the derivative dw/dx, using the Laguerre formula with 6 nodes [29].

Equation (C.11) was solved using a computer as follows. We assigned the quantum numbers n, l, j and the value of E_{nlj} From 0 to the point x_1, the analytical expression (C.12) was used as the solution. The values of the function (C.12) and its derivative with respect to x of the first order were calculated at the point x_1, and were used for a numerical solution of the complete equation (C.11) using the Runge-Kutta method of fourth order with an automatic selection of the integration steps, with the condition that at each step the relative error in the value of the wave func-

tion and its derivative did not exceed 10^{-5}. The numerical integration was performed from the point x_1 to a distance of 13 fm from the nucleus center. By roughly varying the energy E_{nl_j}, it was found that the number of nodes of the calculated wave function became equal to n+1, including the node at the point x = 0. Then, using the calculation of the relative deviation of the derivative of the wave function, obtained by numerical integration from the derivative of the asymptotic (C.13) or (C.14), we found a more exact value of the eigen energy. The calculation of the eigen energy of the level was completed, if the relative deviation of the derivatives at the point where it interlaced with the asymptote, which was a distance of 13 fm from the center of the nucleus, was less than 10^{-3}, or if the absolute error in the value of the eigen energy was less than $5 \cdot 10^{-5}$ MeV. Then the wave function obtained was normalized to unity. To find one value of the eigen energy, from 15 to 23 iterations were necessary. The values of the wave function corresponding to the values of the argument 13 x_i, where x_i were the nodes of the quadratic formula $\int f(x)\,dx = \sum_i A_i f(x_i)$ [30], $i = 1 \div 14$ were calculated and written on magnetic tape, since they were necessary to calculate the integrals $R_{n_1 l_1 j_1 | n_i l_i j_i}$ and $R_{p l_f | n_i l_i j_i}$ from expressions (2.10) and (2.17). /35

To correct the program, we calculated the wave function and the eigen energies of the nucleus of ^{208}Pb with the potential parameters from the study of Blomqvist and Wahlborn [28]. The results obtained fully coincided with their results.

2. Continuous spectrum

The states of the continuum were described by wave functions obtained by solving the Schroedinger equation with the same potential which was used to calculate the wave functions describing the connected states. One difference was that, to reduce the computational time, the spin-orbital term in the potential was discarded. In addition, we only calculated the wave functions with $l \leq 10$.

The correction showed that the states with large ℓ did not make a great contribution to the cross section in the examined region of the neutrino energy.

The equation for the radial parts of the wave functions of the continuous spectrum $\psi_{p\ell_j}(x)$ of a nucleon with the energy E, after substitution of $y_{p\ell}(x) = x\,\psi_{p\ell}(x)$, was obtained from (C.11), if we make the substitution $E_{n\ell_j} - E > 0$, and discard the spin-orbital term in the potential: /36

$$y''_{p\ell}(x) - \frac{\ell(\ell+1)}{x^2} y_{p\ell}(x) + 0{,}04823\left[E + V_0 f_0(x)\right] y_{p\ell}(x) - \qquad \text{(C.15)}$$

$$- 0{,}06939\,(Z-1)\,\frac{\zeta(x)}{x}\,y_{p\ell}(x) = 0 .$$

In the asymptotic region from (C.5) we obtain the equation for Coulomb wave functions $F_\ell(x)$ and $G_\ell(x)$ [15].

Close to the center of the nucleus, (C.15) has the solution (C.12) where the expression for β is obtained from the previous substitution $E_{n\ell_j} \to E$.

The expression (C.12) was selected as the wave function in the region from 0 to the point x_1, and from the point x_1 to a distance of 13 fm from the center of the nucleus the equation (C.15) was solved numerically by the Runge-Kutta method with a constant step. The step was chosen so that their lengths did not exceed 0.1 fm, and was constant in the intervals of $13 x_i + 13 x_{i+1}$, where x_i are the nodes of the quadratic formula, just as in the case of the wave functions of the discrete spectrum. There had to be an integer number of integration steps in these intervals. When these conditions were observed, the integration accuracy was sufficient, and the values of the function calculated at the points $13\,x_i$, after they were multiplied by the number m, determined from the interlacing condition with the asymptote, were written on magnetic tape. A distance of 13 fm from the center of the nucleus, the numerical solution was interlaced with the asymptote, which was selected in the form [15]:

$$2i e^{-i\delta_\ell}\left[F_\ell(x) + iG_\ell(x) + e^{2i\delta_\ell}\left(F_\ell(x) - iG_\ell(x)\right)\right] =$$
$$= 4i\left[\cos\delta_\ell \cdot F_\ell(x) + \sin\delta_\ell \cdot G_\ell(x)\right]. \qquad (C.16)$$

/37

Since we have not considered the imaginary part of the potential, the phase of the scattering δ_ℓ is real. The quantity m, which must be multiplied by the wave function, obtained by numerical integration, and the phase δ_ℓ are determined from the interlacing conditions:

$$m y_{p\ell}(x) = 4i\left[\cos\delta_\ell \cdot F_\ell(x) + \sin\delta_\ell \cdot G_\ell(x)\right], \qquad (C.17)$$

$$\frac{y'_{p\ell}(x)}{y_{p\ell}(x)} = \frac{\cos\delta_\ell \cdot F'_\ell(x) + \sin\delta_\ell \cdot G'_\ell(x)}{\cos\delta_\ell \cdot F_\ell(x) + \sin\delta_\ell \cdot G_\ell(x)}. \qquad (C.18)$$

3. Calculation of integrals and special functions

The integrals $R_{n_f\ell_f j_f J n_i \ell_i j_i}$ and $R_{p\ell_f J n_i \ell_i j_i}$ included in expressions (2.10) and (2.17) were calculated. The integral from 0 to oo was represented in the form of the sum of two integrals, and the first had integration limits from 0 to 13 fm. It was calculated using the quadratic Gauss formula with 14 nodes, using the values of the wave functions written on magnetic tape. The second integral with limits from 13 fm to oo was calculated using the asymptotic expressions (C.13), (C.14) and (C.16) for the wave functions. Since expression (C.13) contains the exponent with negative index, this integral may be readily transformed to the form $\int f(x) e^{-x} dx$, after which it is calculated using the quadratic Laguerre formula with 5 nodes.

The Coulomb wavefunctions, the spherical Bessel functions, the Klebb-Jordan coefficients used in the study, were calculated using specially written programs, whose correctness was verified using

well-known tables of corresponding values.

REFERENCES

/38

1. H. Überall, B. A. Lamers, J. B. Langworthy, F. J. Kelly. Phys. Rev. C6 (1972), 1911.

2. J. S. O'Connel, T. W. Donnelly, J. D. Walecka. Phys. Rev., C6 (1972), 719.

3. J. B. Langworthy, B. A. Lamers, H. Überall. Nucl. Phys., A280 (1977), 351.

4. T. W. Donnelly, J. D. Walecka. Phys. Letters, B41 (1972), 275.

5. G. V. Domogatskiy, R. A. Eramzhyan. Izvestiya Akademii Nauk SSSR, seriya fizicheskaya, 41, 1977, 1969.

6. W. A. Landford, B. H. Wildenthal. Phys. Rev. Letters, 29, (1972), 608; B. H. Wildenthal, et al., Phys. Rev., C4, (1971), 1266.

7. G. S. Bisnovatyy-Kogan, M. A. Rudzskiy, Z. F. Seidov. ZhETF, 67, 1974, 1621.

8. J. Bell, C. H. Llewellyn Smith. Nucl. Phys., B28 (1971), 317.

9. Ya. B. Zel'dovich, O. Kh. Guseynov. Doklady Akademiix, Nauk SSSR, 162, 1965, 711.

10. D. K. Nadjozhin. Astrophys. and Space Sci., 51 (1977), 283.

11. E. V. Bugayev, G. S. Bisnovatyi-Kogan, M. A. Rudzskyi, Z. F. Zeidov, in Neutrino-77 Proceedings of the International Conference on Neutrino Physics and Neutrino Astrophysics, ed. M. Markov, p. 193, Nauka, Moscow, 1978.

12. I. D. Walecka, in Muon Physics, ed. by V. W. Hughes and C. S. Wu (Academic Press N.Y., 1975).

13. F. Cannata, R. Leonardi. Phys. Rev., C5 (1972), 1189.

14. R. H. Dalitz, D. R. Yenni. Phys. Rev., 105 (1957), 1598.

15. A. G. Sitenko. Lectures on scattering theory. Kiev, "Vishcha shkola", 1971.

16. D. Freedman. Phys. Rev. D9 (1977), 1989.

17. S. Weinberg. Phys. Rev., D5 (1972), 1412; A. Salam. In Elementary Particle Theory, ed. by N. Svartholm (Almqvist, Stockholm, 1968). /39

18. Luyten, T. R., H. P. Rood, H. A. Tolhoek. Nucl. Phys., 41 (1963), 236.

19. S. S. Gershteyn, Ya. B. Zel'dovich. ZhETF, 29, 1955, 698.

20. C. J. Christensen, A. Niclsen, A. Bahnsen, W. K. Brown, B. M. Rustad. Phys. Lett., 26B, (1967), 11.

21. S. I. Bilen'kaya, Yu. M. Kazarinov, L. I. Lapidus. ZhETF, 60, 1971, 460.

22. R. L. Kustom, D. E. Lundquist, T. B. Novey, A. Yokasawa and F. Chilton. Phys. Rev. Letters, 22, (1969), 1014.

23. S. D. Drell, C. Schwartz. Phys. Rev., 112, (1958), 568.

24. I. Ayzenberg, V. Grayner. Mekhanizmy vozbyzhdeniya yadra (Mechanisms of nucleus excitation), Moscow, Atomizdat, 1973.

25. D. A. Varshalovich, A. N. Moskalev, V. K. Khersonskiy. Kvantovaya teoriya uglovogo momenta (Quantum theory of angular momentum), Leningrad, Nauka press, 1975.

26. C. J. Batty, G. W. Greenless. Nucl. Phys. A133, (1969), 673.

27. L. P. Lapina. Preprint LIYaF, No. 241, Leningrad, 1976.

28. I. Blomqvist, S. Wahlborn. Arkiv.Phys. 16, (1960), 545.

29. V. I. Krylov, L. T. Shul'gina. Spravochnaya kniga po cheslenomu integrerovaniyu (Handbook on numerical integration), Moscow, Nauka press, 1966.

30. A. D. Kronrod. Uzly i vesa kvadraturnykh formul (Nodes and weights of quadratic formulas), Moscow, Nauka press, 1964.

TABLE 1

PARAMETERS OF THE POTENTIAL WS USED IN THIS STUDY

Nucleon	r_0, f	a_0, f	r_s, f	a_s, f	V_s, MeV
Neutron	I,36	0.73	I.26	0,60	6.99
Proton	I.28	0.76	I,09	0.60	5.78

TABLE 2

EIGEN ENERGIES OF THE CONNECTED STATES OF THE NUCLEI *)

Ядро		$1s_{1/2}$	$1p_{3/2}$	$1p_{1/2}$	$1d_{5/2}$	$2s_{1/2}$	$1d_{3/2}$	$1f_{7/2}$	$2p_{3/2}$	$2p_{1/2}$	$1f_{5/2}$	$1g_{9/2}$	$2d_{5/2}$	$3s_{1/2}$	$2d_{3/2}$	$1g_{7/2}$
^{12}C***	n	36.16	24.44	9.38	12.77	4.87	0.84									
	p	32.99	21.61	6.64	10.25	2.68										
^{16}O***	n	35.91	23.20	18.87	10.49	7.99	3.79									
	p	26.44	14.14	10.03	2.14	1.56										
^{37}Cl	n	34.54	25.91	23.51	16.75	13.41	12.00	7.22	7.36	2.79	0,64					
	p	36.85	26.99	24.19	16.41	12.99	11.45	5.32	2.68	1.25						
^{56}Fe	n	37.55	30.33	28.70	22.44	19.15	18.91	14.02	10.21	8.52	8.39	5.19	2.05	1.52	0.21	
	p	37.31	29.26	27.17	20.34	16.70	16,29	10.71	6.75	5.25	4.90	0.54				
^{71}Ga	n	36.38	30.08	28.76	23.11	20.03	20.17	15.60	11.78	10.22	10.73	7.63	3.91	2.89	1.89	1.01
	p	38.26	31.13	29.40	23.11	19.48	19.61	14.32	9.97	8.52	9.03	4.89	0.82			
^{81}Br	n	36.60	30.72	29.57	24.18	21.21	21.56	17.08	13.27	11.80	12.65	9.52	5.52	4.24	3.43	3.27
	p	38.18	31.57	30.02	24.07	20.49	20.86	15.79	11.33	9.93	10.82	6.83	2.31	0.91	0.42	0.41

* The table gives the values in MeV for the quantities $|E_{nlj}|$.

** The eigen energies are found in the potential (C.1)-(C.5) with the parameters (C.6), (C.7).

*** The eigen energies are found in the potential (C.1)-(C.5) with the values $V_{on} = 56$, $V_{op} = 52$.

The remaining parameters were taken from Table 1.

HEADINGS FOR THE FIGURES

Fig. 1. Total cross section of reactions (1.1) and (1.2) for ^{12}C. The solid lines show the sum σ_{gg+gH} of total cross sections gg and gH positions. The numbers 1,2,3 designate the cross sections of the n-p, n-n and p-p transitions. The dashed lines show the cross sections of the gg transitions. The crosses show the cross section for the reaction (1.1) according to [7].

Fig. 2. The same as for Fig. 1, but for the nucleus ^{16}O.

Fig. 3. The same as for Fig. 1, but for ^{37}Cl.

Fig. 4. The same as for Fig. 1, but for ^{56}Fe.

Fig. 5. The same as for Fig. 1, but for ^{71}Ga.

Fig. 6. The same as for Fig. 1, but for ^{81}Br.

Fig. 7. Comparison of the total cross section σ_{gg+gH} of the reaction (1.1) for ^{16}O, obtained in this study, with the results of other authors. The numbers designate: 1 - the study; 2 - cross section from [3]; 3 - cross section obtained in the Fermi-gas model [12]; 4 - cross section from [8]; 5 - cross section for a free neutron [12], multiplied by 8; the crosses -- cross section according to [7].

Fig. 8. Comparison of the cross section σ_{gg+gH} (solid line) and σ_{gg} (dashed line) of this article with the transition cross section considering all individual levels from [1] (dot-dashed line).

Fig. 9. Comparison of the reduced cross section σ_{gg+gH}/N with the cross section for a free neutron [for the reaction (1.1)].

Fig. 10. Comparison of the angular dependences $d\sigma/d\Omega$ for ^{16}O in in different models: 1 - this article; 2 - Fermi-gas model [12]; 3 - [8]; 4 - free neutron. The graphs are compiled for E_ν = 300 MeV [the reaction (1.1)]. /43

Fig. 11. Reduced differential cross sections $(d\sigma/d\Omega)/N$ for all nuclei examined and $d\sigma/d\Omega$ for a free neutron; E_ν = 300 Mev.

Fig. 12. Quasi-elastic peaks $d^2\sigma/d\Omega\, dE_e$ for the reaction with ^{16}O. The solid lines show the quasi-elastic peaks obtained in this article; dashed lines -- in the Fermi-gas model [12]. The numers around the curves designate the quantity $\sin^2\theta/2$, where θ is the angle between the neutrino and the electron. The neutrino energy equals 300 MeV.

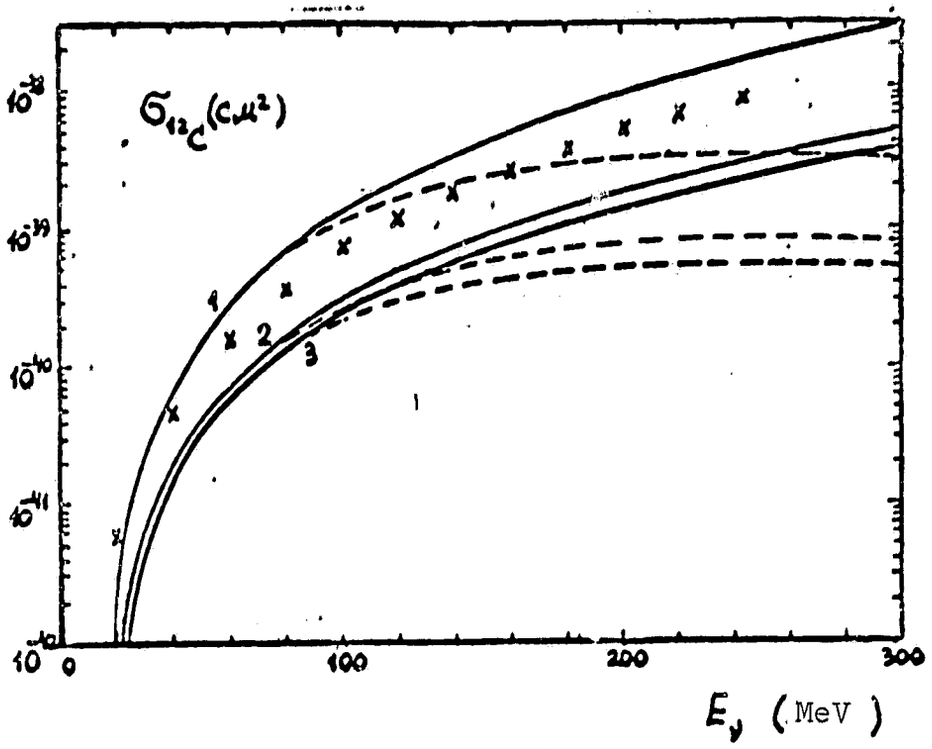
$\sigma_{^{12}C}(cm^2)$
10^{-38}
10^{-39}
10^{-40}
10^{-41}
10^{-42}
0
100
200
300
E_ν (MeV)
1
2
3

Fig. 1

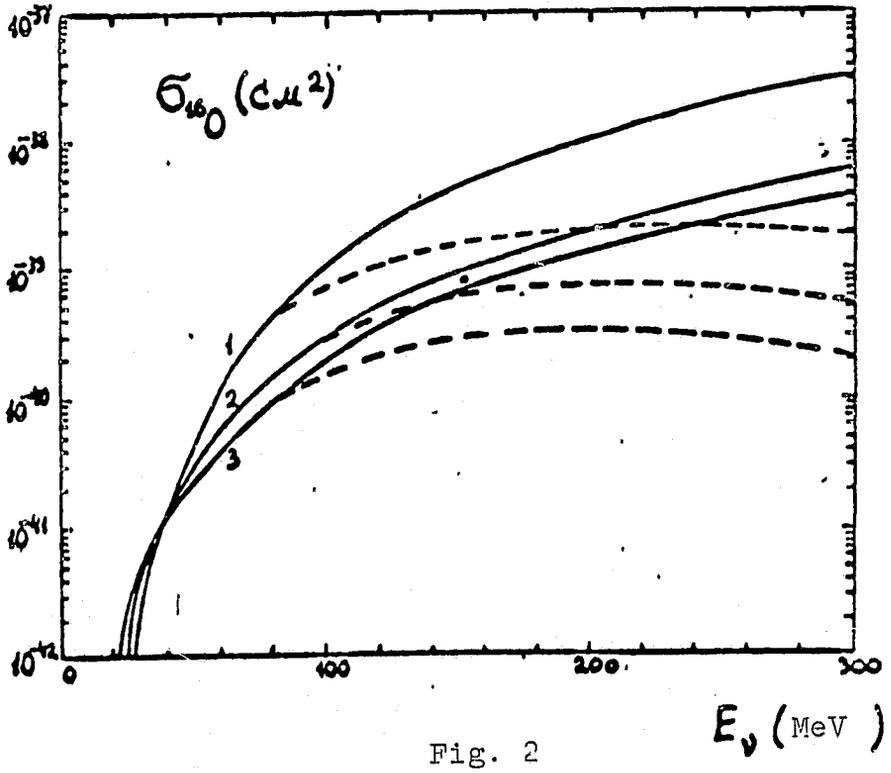
$\sigma_{^{16}O}(cm^2)$
10^{-37}
10^{-38}
10^{-39}
10^{-40}
10^{-41}
10^{-42}
0
100
200
300
E_ν (MeV)
1
2
3

Fig. 2

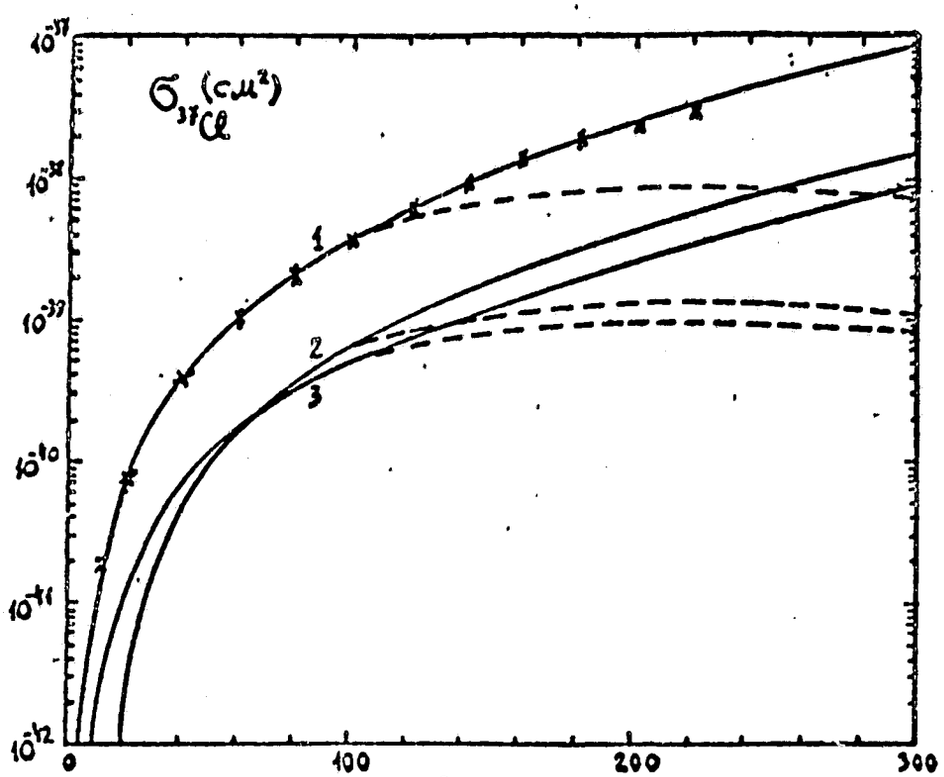
$\sigma_{^{37}Cl}$ (см²)
1
2
3
0
100
200
300
E_γ (MeV)

Fig. 3

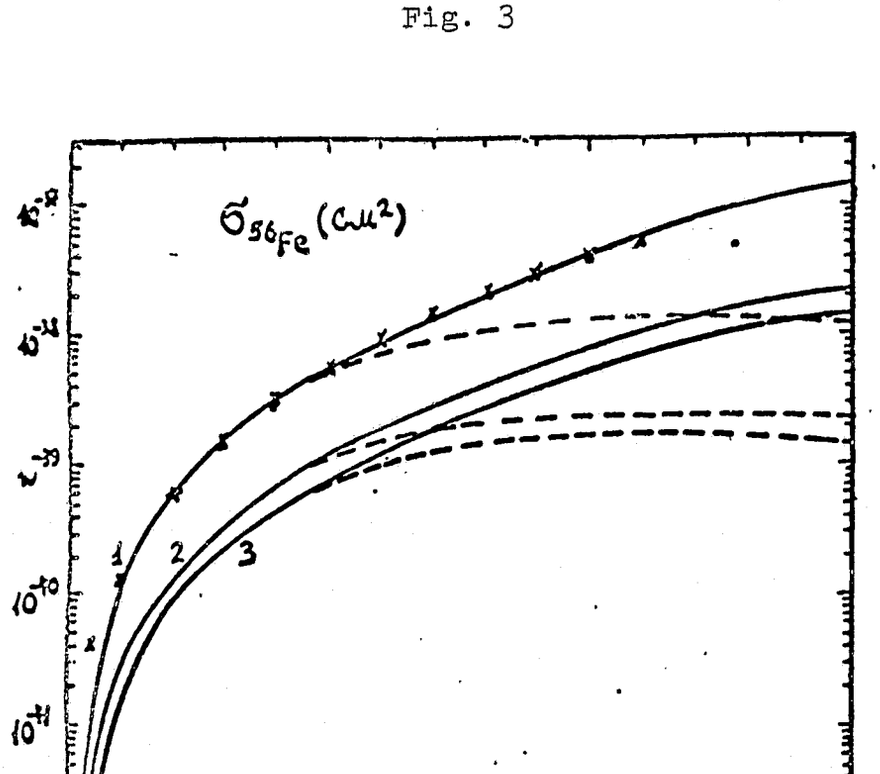
$\sigma_{^{56}Fe}$ (см²)
1
2
3
0
400
200
300
E_γ (MeV)

Fig. 4

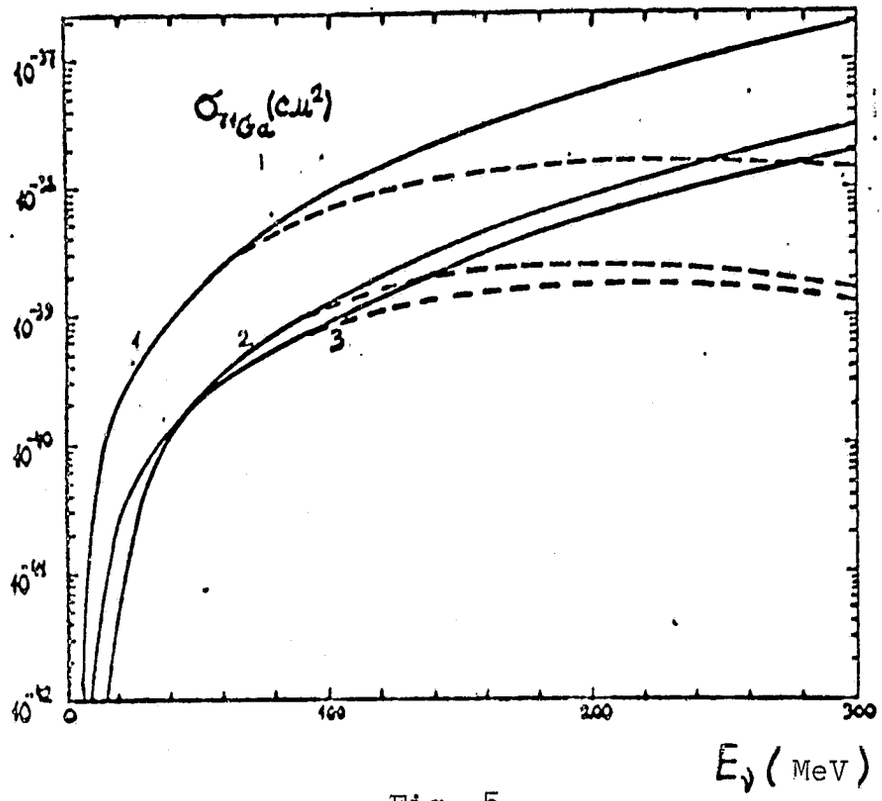
$\sigma_{\nu^{71}Ga}(cm^2)$
1
2
3
10^{-37}
10^{-38}
10^{-39}
10^{-40}
10^{-41}
0
100
200
300
E_ν (MeV)

Fig. 5

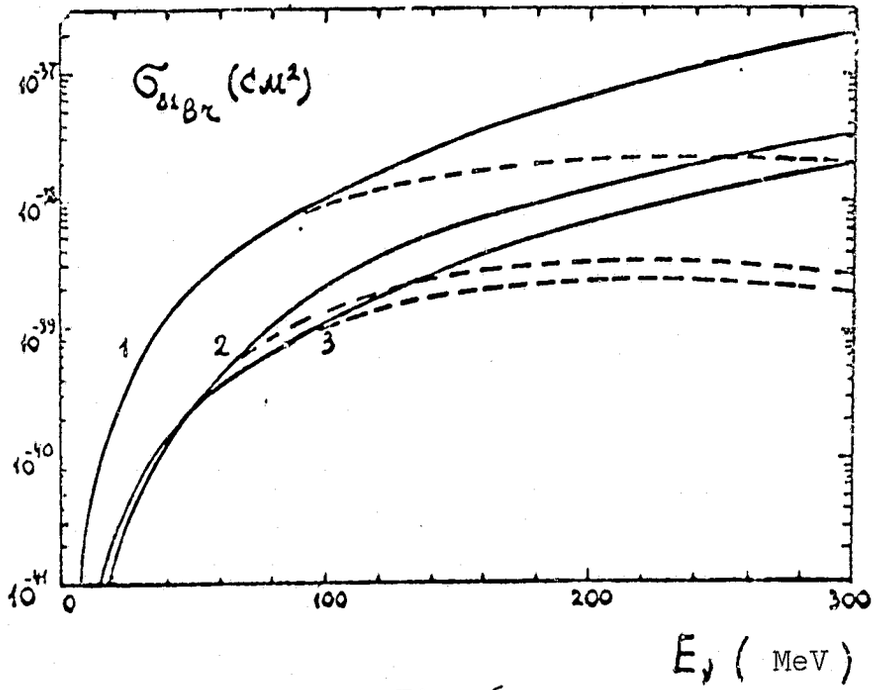
$\sigma_{\nu^{81}Br}(cm^2)$
1
2
3
10^{-37}
10^{-38}
10^{-39}
10^{-40}
10^{-41}
0
100
200
300
E_ν (MeV)

Fig. 6

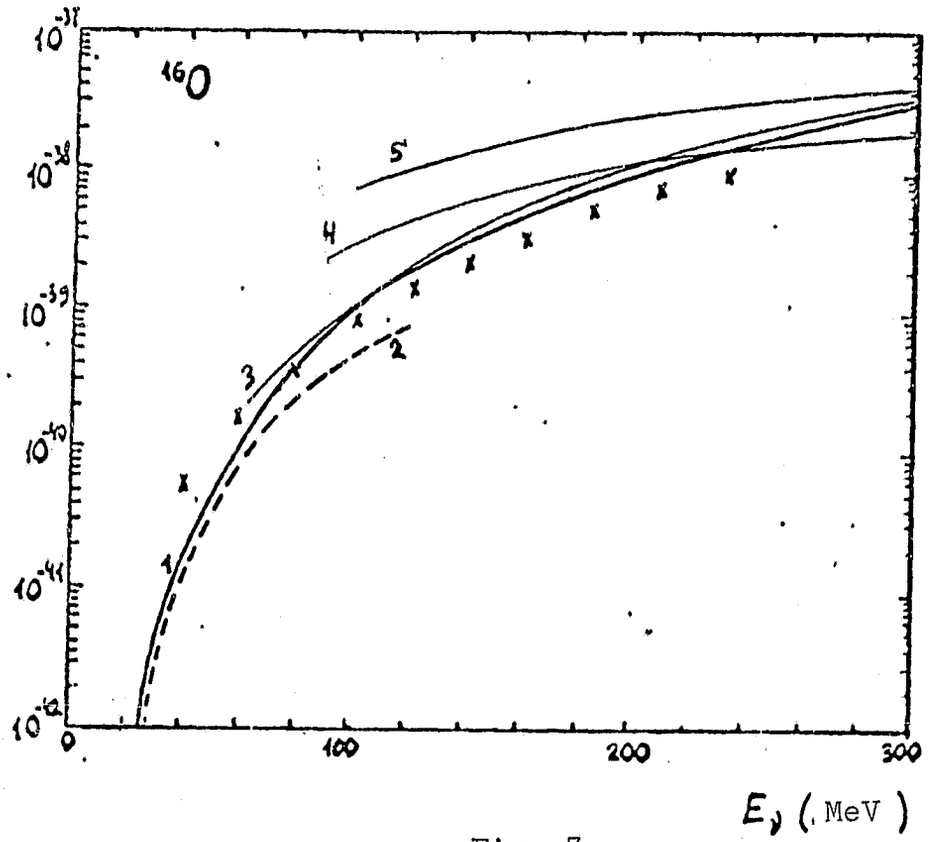
10^{-37}
^{16}O
10^{-38}
10^{-39}
10^{-40}
10^{-41}
10^{-42}
5
4
3
2
1
0
100
200
300
E_γ (MeV)

Fig. 7

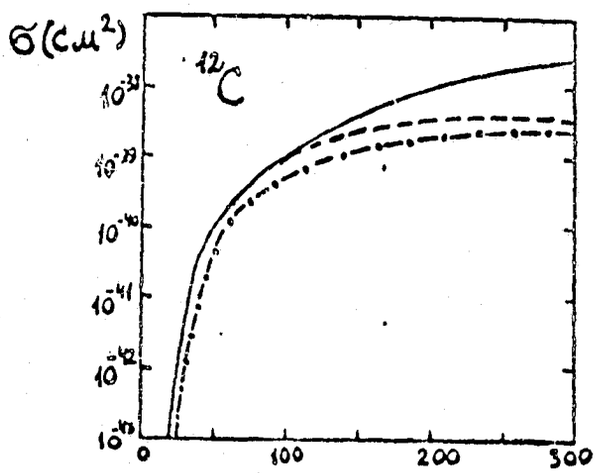
$\sigma(cm^2)$
^{12}C
10^{-39}
10^{-40}
10^{-41}
10^{-42}
10^{-43}
0
100
200
300
E_γ (MeV)

Fig. 8

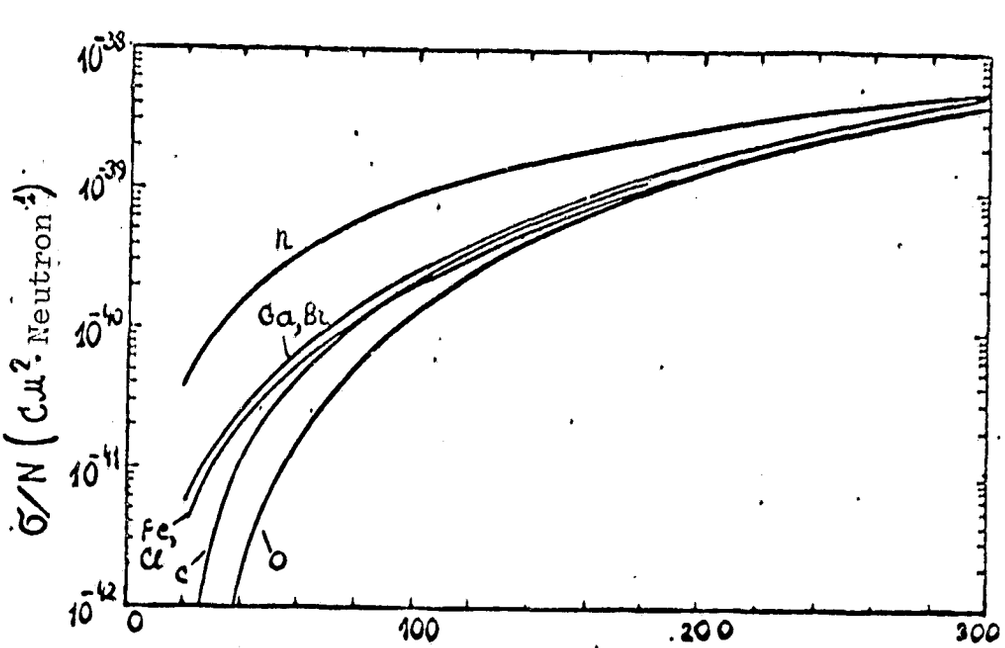
10^{-38}
10^{-39}
10^{-40}
10^{-41}
10^{-42}
σ/N (см^2. Neutron^{-1})
n
Ca, Br
Fe, Cl
O
0
100
200
300
E_γ (MeV)

Fig. 9

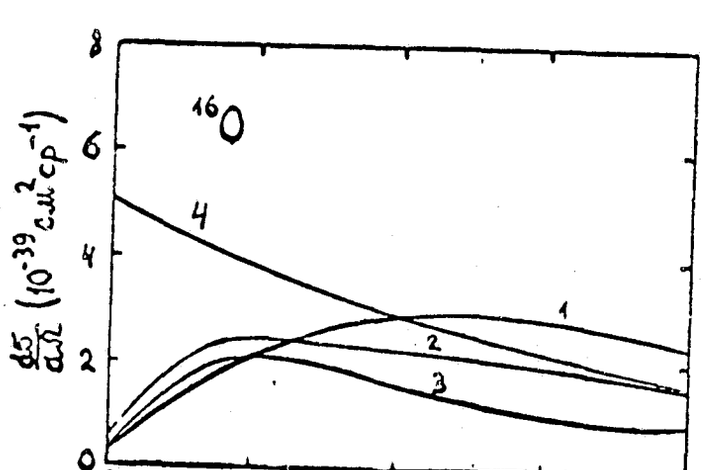
8
6
4
2
0
^{16}O
4
1
2
3
0
0.25
0.5
0.75
1.0
$\frac{d\sigma}{d\Omega}$ (10^{-39} см^2 ср$^{-1}$)
$Sin^2\frac{\theta}{2}$

Fig. 10

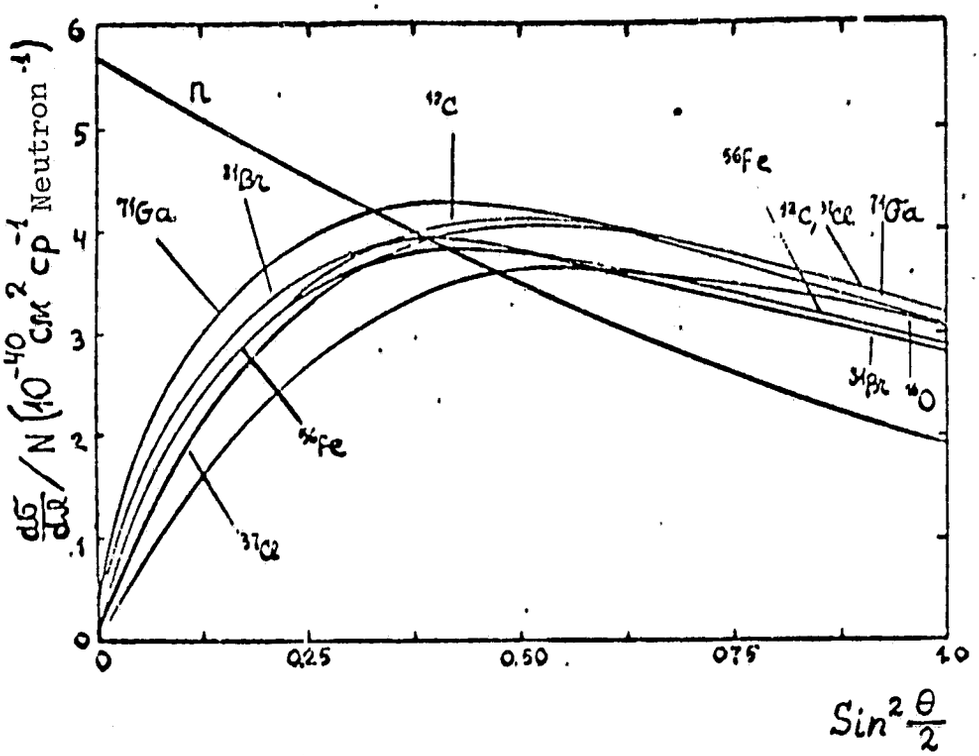
n
^{12}C
^{56}Fe
^{81}Br
^{71}Ga
$^{12}C, ^{35}Cl$
^{71}Ga
^{81}Br
^{16}O
^{56}Fe
^{37}Cl
$\frac{d\sigma}{d\Omega}/N\ (10^{-40}\ cm^2\ cp^{-1}\ Neutron^{-1})$
$Sin^2\frac{\theta}{2}$

Fig. 11

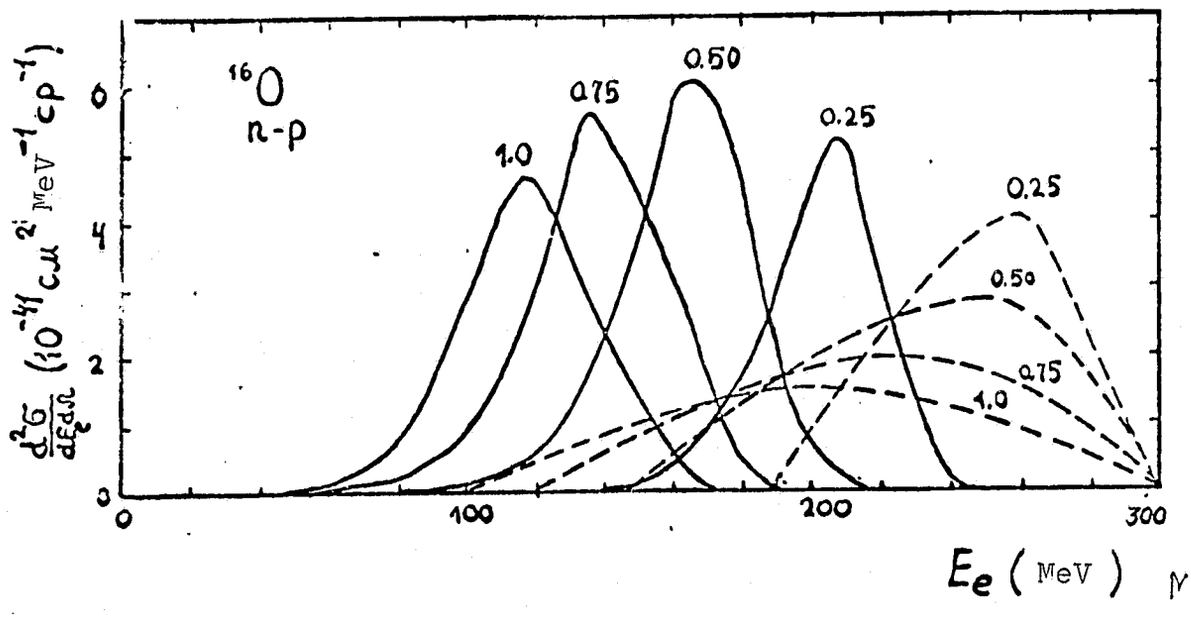
^{16}O
n-p
1.0
0.75
0.50
0.25
0.25
0.50
0.75
1.0
$\frac{d^2\sigma}{dE_e d\Omega}\ (10^{-41}\ cm^2\ MeV^{-1}\ cp^{-1})$
E_e (MeV)

Fig. 12